A 5MW direct-drive generator for floating spar-buoy wind turbine: Development of a fully-coupled Mechanical model

A 5MW direct-drive generator for floating spar-buoy wind turbine: Development and analysis of a fully coupled Mechanical model

Latha Sethuraman, Yihan Xing, Zhen Gao, Vengatesan Venugopal, Markus Mueller and Torgeir Moan

Proceedings of the Institution of Mechanical Engineers, Part A: Journal of Power and Energy published online 5 June 2014
DOI: 10.1177/0957650914537262

Original Article

Institution of MECHANICAL ENGINEERS
Journal of POWER AND ENERGY

Proc IMechE Part A:
J Power and Energy
0(0) 1–24

DOI: 10.1177/0957650914537262
pia.sagepub.com
SAGE

A 5MW direct-drive generator for floating spar-buoy wind turbine: Development and analysis of a fully coupled Mechanical model

Latha Sethuraman[1], Yihan Xing[2], Zhen Gao[2], Vengatesan Venugopal[1], Markus Mueller[1] and Torgeir Moan[2]

Abstract

This work forms the first of a two-part investigation aimed at identifying the challenges and opportunities of implementing a direct-drive generator for a spar-buoy type floating wind turbine. Preliminary specifications are presented for a fully coupled aero-hydro-servo-elastic model of a floating wind turbine with a 5 MW direct-drive generator. The drive-train model uses a low-speed, high-torque radial flux permanent magnet generator supported by two main-shaft bearings. The mechanical properties of the drive-train, including the main dimensions, mass of major nacelle equipment and details for the hub/nacelle assembly are presented. The rationale behind the adjustments to the tower and platform properties and the motivation to selection of best arrangement that is appropriate for supporting the developed system is explained. A discussion on the development of the variable speed-variable pitch control system suitable for the direct-drive system including modifications to avoid negative damping and blade-pitch instability are presented. Fully coupled simulations for the developed aero-hydro-servo elastic model were carried out in HAWC2 for the normal operating conditions of the wind turbine. The aerodynamic response of the model was verified and compared with that of a geared floating wind turbine system. Some initial results comparing the main shaft loads of the land-based and floating versions of the direct-drive wind turbine suggest satisfactory dynamic behaviour of the drive-train. The results prompt further research using a detailed drive-train model to verify the internal response, loading and durability of the components to assess their compatibility with a floating wind turbine system.

Keywords

Floating wind turbine, direct-drive generator, drive-train, controller, tower, platform

Date received: 23 October 2013; accepted: 28 April 2014

Introduction

In recent years, there has been a growing interest in the research on floating wind turbines (FWTs) with several new concepts emerging.[1] The spar-buoy wind turbine has been extensively researched with several studies aimed at understanding and improving their global dynamic response.[2–6] These studies have emphasised the importance of fully coupled dynamics solution for floating wind turbines providing little or no information on the impact or dynamics of drive-train. As the success of the system lies in the compatibility and performance of the drive-train, there is a need for more research in this subject area. A survey of drive-train architecture for floating wind turbines shows the geared drive-train as the most standard concept.[7] These designs promise to be the most lightweight construction, yet reliability is still a major concern with many gaps in the design process leading to premature failure of gearbox and its components.[8] Recent studies have pointed out greater fatigue loads and, therefore, greater cost implications with the geared drive-train when applied for FWTs.[9,10]

Drive-train designers are constantly exploring new alternatives to improve the reliability and performance.[11] Current trends are towards gearless drive-trains, which can be made smaller for higher rotational speeds. In gearless drive-trains, the rotor hub is directly coupled to the generator that operates

[1]Institute for Energy Systems, The University of Edinburgh, Edinburgh, UK
[2]Department of Marine Technology, Norwegian University of Science and Technology, Trondheim, Norway

Corresponding author:
Latha Sethuraman, School of Engineering, The University of Edinburgh, The King's Buildings, Edinburgh, EH9 3JL, UK.
Email: L.Sethuraman@sms.ed.ac.uk

at a low speed. But the downside to using such a direct-drive generator is twofold: cost and weight. Previous literature suggests good prospects for direct-drive generators when employed for floating wind turbines.[7,12,13] However, ensuring competitiveness, reliability and robust operation of such a drive-train requires an understanding of detailed dynamic behaviour of the drive-train considering the aerodynamic interaction, platform motions and control system response.

To facilitate early conceptual studies, preliminary design specifications were developed for a fully coupled aero-hydro-servo-elastic model of 5 MW floating wind turbine system that could support a direct-drive generator (henceforth referred to as FWTDD system). The model presented here is useful for performing fully coupled time-domain analyses using multi-body simulation codes such as HAWC2[14] and SIMPACK.[15] Details of the drive-train, including mass and mechanical properties, layout of the nacelle, control-system properties are presented. The important challenges in dealing with large nacelle mass, adjustments to tower and platform properties and the rationale behind development of the optimal system are discussed. The behaviour of the model was verified for the normal operating conditions of the wind turbine and compared with that of a geared FWT system; some initial results on the main shaft loading are presented and compared with a land-based direct-drive wind turbine.

Direct-drive generators for floating wind turbines

Several topologies of direct-drive generators for wind turbines have emerged in recent years; these include electrically excited synchronous generator (EESG), permanent magnet synchronous generator (PMSG) and squirrel cage induction generator (SCIG) configurations.[16] Amongst these, PMSGs hold the largest market share.[17] The relative flexibility of their design allows for modular lighter weight constructions designed as iron cored or core-less constructions with flux path in the radial, axial or transverse directions.[18] An SWOT analysis by Leban et al.[12] highlights greater optimising potential for radial flux and transverse flux PMSGs. Paulsen et al.[19] investigated a 5 MW transverse flux direct-drive generator for a vertical axis floating wind turbine. The generator had a substantially large air-gap diameter and pole count. This is perfectly acceptable for vertical axis FWT systems because the generators have lesser mechanical restrictions, and can be located closer to the centre of gravity of the system where the motion induced loads are substantially reduced. Whereas, implementing such a large generator for horizontal axis FWTs will be much more challenging.[7] Research on ironless direct-drive generators is also gaining momentum in an effort to enable FWT technology rated above 5 MW.[13,20] These designs suggest significant cost and weight advantages, yet are in their experimental phases of development. Also, with greater complexity in design and manufacturing, the robustness of these designs entirely relies on the effectiveness of stator-rotor air-gap control, which can be difficult especially at higher magnitude nacelle accelerations.

Sethuraman et al.[7] identified the radial flux iron-cored PMSG as a prospective candidate for an FWT system when compared to axial and transverse flux configurations due to its simple structure, shorter load path and relative simplicity in air-gap control. From the view of rotor position, there are outer rotor type and inner rotor type PMSG. Based on the mounting mode of the PM on the rotor, there are surface mounted type and embedded type PM machines. The inner rotor machine with surface-mounted magnets seems to be an interesting choice due to higher air gap flux density and better thermal management as compared to outer rotor configuration. Preliminary studies on an inner rotor radial flux PMSG for a FWT system by Sethuraman et al.[21] emphasised the need for greater understanding of the dynamics of the drive-train and potential opportunities for further research. Hence, the radial flux PMSG with inner rotor construction was chosen as the topic for this research.

Specifications for the fully coupled mechanical model

Different options exist for bearing types and arrangements for radial flux PMSGs.[22–24] As drive-train parameters for the chosen radial flux topology was not available at the time of the study, it was decided to develop these parameters. The model for a 5 MW system developed Jonkman[25] was adapted with changes to the nacelle, drive-train and control system properties to allow the integration of a direct-drive generator. The aerodynamic and blade structural properties for the turbine and hub design were retained as the NREL offshore 5 MW baseline wind turbine.[25,26] Mooring properties were retained from Karimirad and Moan,[4] but modifications to the tower, support platform properties and controller were necessary. The following sections provide details of the drive-train and document the preliminary specifications for the important elements of the FWTDD system in the same order as described by Jonkman.[25] Wherever appropriate, the properties for the baseline system are listed alongside to highlight the differences between the two systems. Where the properties are not listed, the relevant values from baseline system[25] are applicable.

Direct-drive generator topology

The direct-drive generator considered for this study is a low-speed radial flux permanent magnet generator

of the interior rotor construction obtained from an optimisation study.[27] The rotor is a cylinder of disc-type construction; stator is also a cylinder with double spider arrangement. Figure 1 provides an illustration of the rotor nacelle assembly for the direct-drive generator and constructional details (clearances). The main properties of the machine based on the study of Bang and Polinder[28] are summarised in Table 1. The hub was assumed to be integrated to the main shaft, which carries the generator rotor. The turbine-rotor and the shaft are supported by means of two roller bearings BR1 and BR2 that are housed on generator stator support structures. Shaft loads are transferred from the generator rotor to the stator through the BR1, BR2 and stator support arms. The stator is integrated to the bedplate that is coupled to the tower by means of a yaw system. Hub thrust, shear and bending moments are transferred to the nacelle bedplate by the main bearings via the stator support structure. The topology is similar to the commercially available MTorres design.[29] BR-1 is a cylindrical roller bearing (CRB) designed to take radial loads; BR-2 is a double row tapered roller bearing with inner race (TDI) designed to carry both the axial loads and radial loads. This configuration was chosen to be more efficient in terms of stiffness-to-mass ratio[30] and was based on the recommendations from bearing manufacturer, TIMKEN.[31] It is emphasised that the bearing arrangement/locations were tentative and not optimised for the design. For simplicity, any other components of drive-train mounting system such as suspension or shaft coupling elements are not shown.

Development of drive-train mechanical properties

For this study, the implemented control algorithm regulates the generator torque and the rotor speed, therefore, the first eigen mode for torsional compliance in the drive-train (variable rotor speed and drive-shaft flexibility) was of most interest. Previous studies considering torsional model for global analysis have

Table 1. Generator properties.

Item Generator type	Units	Value/Description Radial flux PM, interior rotor
Generator nominal power	MW	5.56
Rated torque	MN-m	4.38
Efficiency	%	96.6
Rotor diameter	m	6.36
Stator diameter	m	6.37
Axial length	m	1.72
Air-gap length	mm	6.36
Magnet height	mm	15.9
Rotor mass	kg	51,440
Stator mass	kg	77,040

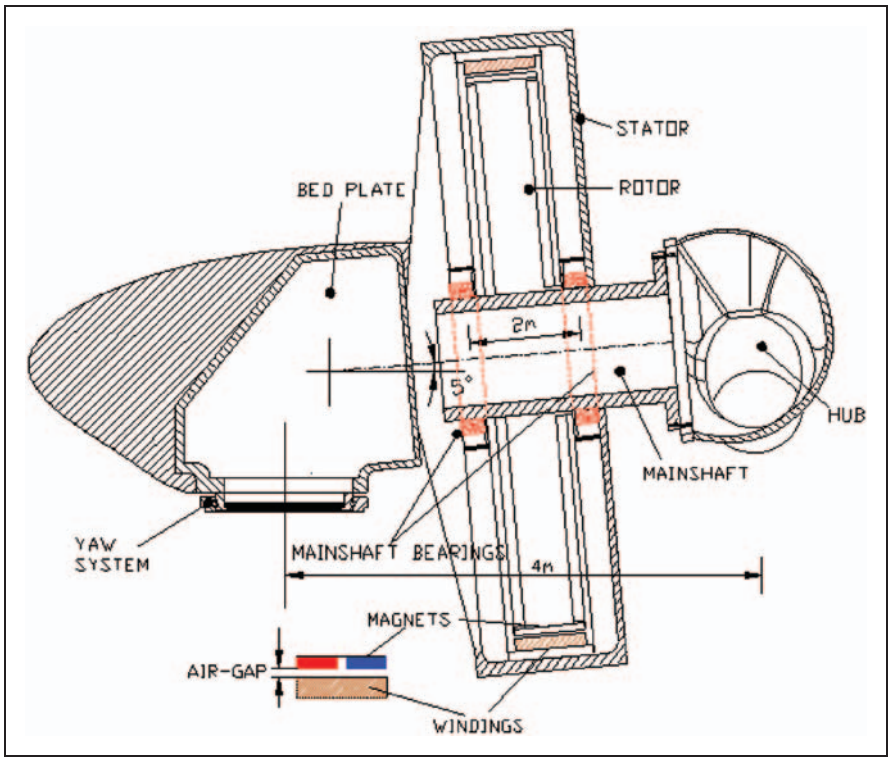

Figure 1. Rotor nacelle assembly of a direct-drive generator.

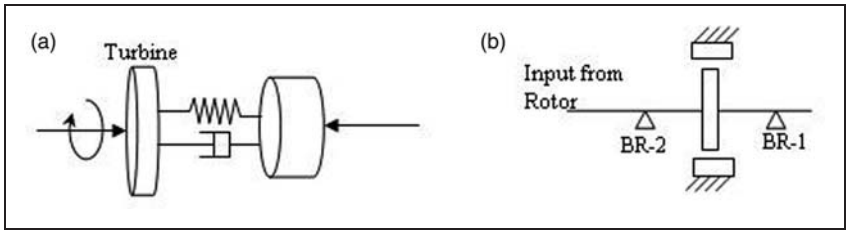

Figure 2. (a) Simple mechanical model of a direct-drive generator; (b) direct-drive generator topology.

Table 2. Drive-train mass and dimensions.

Item/Description	Units	NREL, 5 MW baseline[33–35]	Scaling law model for direct-drive system[33]	Parametric design data (extrapolated for 5 MW direct drive)[23]	Estimated dimensions/weights for FWTDD system
Shaft mass	ton	17.38	–	9.4	13.24
Shaft length	m	3.76	3.78	2.03	3
Shaft outer diameter	m	1	–	1	1
Shaft inner diameter	m	0.5	–	0.5	0.5
Generator housing mass/ mainframe mass	ton	28.24[33]	15.53	15.33	15.33
Main shaft bearing mass	ton	2.7	2.7	0.1	2.7

FWTDD: floating wind turbine with a direct-drive generator.

shown to be adequate for most calculations providing reasonable conclusions about the overall dynamic behaviour allowing time efficiency and modelling precision.[10,32] This encouraged the consideration of a single DOF torsional spring damper system (refer to Figure 2(a)) with a rigid shaft and generator rotor. The NREL 5 MW baseline wind turbine with a rated rotor speed of 12.1 r/min drives a low-speed radial flux PMSG. The generator inertia about the shaft (3.79×10^5 kgm^2) was comparatively lower than the equivalent geared drive-train value reported in Jonkman et al.[26] In the determination of the mass and dimensions of the rest of the components of the drive-train, a number of reports on drive-train design were reviewed.[23,33–35] Because several arrangements are possible for the shaft-bearing assembly,[22,23] there is no standard formula available to estimate the dimensions of the shaft. However, it is intuitive to expect the shaft to be smaller in length compared to a conventional geared drive-train.

The scaling law model[33] and the parametric design models[23] for the direct-drive generator offered some initial ideas about the shaft dimensions and component weights. The data for the 5 MW geared drive-train were interpreted from Malcolm and Hansen[34] and Kooijman et al.[35] Table 2 summarises the mass estimates from the various models.

The shaft was assumed to be a uniformly hollow cylindrical steel tube made from high-strength characteristic yield of 828 MPa and modulus of rigidity of 79 GPa in line with the study of Malcolm and Hansen.[34] The shaft mass for the FWTDD system by extrapolation[23] was estimated to be 9.4 tons. With the same inner and outer diameters as that of the geared drive-train, this gave a total shaft length of 2.03 m, which appeared to be insufficient for the present direct-drive model having a core length of 1.72 m and total generator axial length greater than 2.0 m including stator support. Therefore, a clearance of 0.5 m on either side of generator was a reasonable assumption to make, resulting in an overall shaft length of 3 m. This gave an estimated shaft mass of 13.24 tons. The value for generator housing mass was assumed from Poore and Lettenmaier[23] and Fingersh et al.[33] The structural adequacy of the shaft was verified by performing a finite element analysis (FEA) in SolidWorks.[36] Column 5 in Table 2 presents the estimated main dimensions and mass properties for the drive-train.

Drive-train mechanical constants

In computing the equivalent drive shaft mechanical constants for the 1 DOF system, contributions to torsional stiffness came from the drive shaft and the generator rotor with negligible stiffness due to electromechanical torque. The magnetic coupling between rotor and stator (grid) of a synchronous generator can be described by a mechanical torsion spring, with negligible damping.[37]

The equivalent torsional stiffness of the drive-train was computed as 2.17 GNm/rad using the standard torsion formula for hollow shafts;[38] this value was at least 2.5 times greater than the geared system. The equivalent drive-shaft torsional-damping

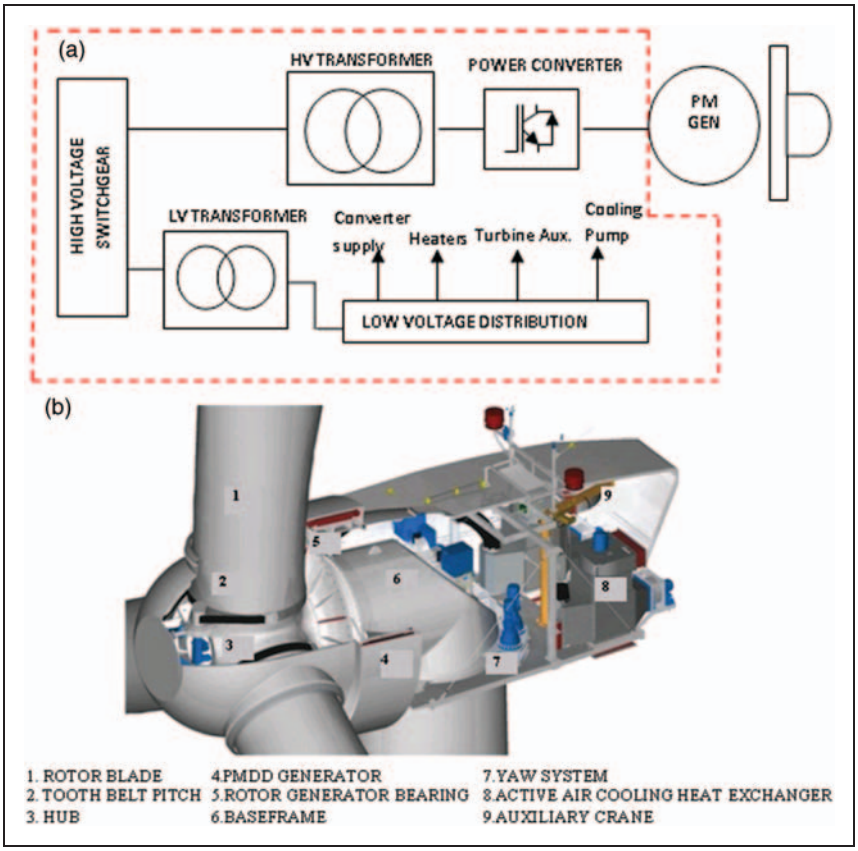

Figure 3. (a) Typical nacelle layout for a direct-drive generator;[40] (b) Typical component layout at the nacelle of a direct-drive generator.[41]

coefficient was computed assuming a structural-damping ratio that was 5% of critical.[26] A large torsional stiffness in the system resulted in larger natural frequencies in the torsional mode for the free–free condition and fixed–free mode (if the generator DOF is disabled).[39] The total mass of the generator (including magnets, windings and steel) was estimated to be about 160 tons. No effort was made to size or optimise the rest of the elements of the drive-train, including ancillary equipment such as yaw drive, nacelle cover, etc., whose masses were assumed from existing models and commercial designs.[13,40] The output of the generator is connected to a dedicated power conversion and distribution equipment that contributes to a further 120 tons.[40] Figure 3(a) and (b) shows the typical component and nacelle layout of a direct-drive generator. The baseline arrangement had the generator converter and transmission equipment at the nacelle.[26] If a similar arrangement was to be adopted for the FWTDD system, then this would result in an overall nacelle mass of 330 tons. Table 3 presents the drive-train properties with column 4 presenting the properties of the baseline system as reference.

Hub and nacelle properties

The hub of the wind turbine was located 4 m upwind of the tower centre line at an elevation of 90 m above the mean sea level. The vertical distance from the tower top to hub was 2.09 m. The elevation of the yaw bearing and shaft tilt were retained as the original baseline system. The vertical distance along the yaw axis from the tower top to the shaft was 1.82 m. The distance directed along the shaft from the hub centre to the main bearing BR2 was taken to be 0.65 m. The hub mass and inertia were retained from the baseline model. The initial estimate for the nacelle CM was located at 0.65 m upwind of the yaw axis and 1.5 m above the yaw bearing. Table 4 summarises the nacelle and hub properties discussed in this section with properties of the baseline system as reference.

The floating spar system

A spar-type FWT system was designed to support the proposed 5 MW direct-drive generator design. This is a ballast stabilised catenary moored spar system with the basic design mentioned in Karimirad and Moan[4] and Jonkman.[25] For the evaluation of the spar properties and ballast requirements, the super-structure (tower, nacelle) design has to be determined. With the knowledge of the nacelle and turbine mass (previous two sections), the tower properties were determined as the first step.

Table 3. Drive-train properties and mass of major equipment.

Item/Description	Units	FWTDD system	NREL, 5 MW baseline system[25,26]
Turbine power	MW	5.0	5.0
Rated rotor speed	r/min	12.1	12.1
Generator speed	r/min	12.1	1173.7
Generator rated torque	MN-m	4.3	0.043
Rotor system layout	–	3-bladed Upwind	3-bladed Upwind
Drive-train	–	Low speed, Direct drive, radial flux PMSG	High speed, Multi-stage Gearbox, Induction generator
Electrical generator efficiency	%	96.6	94.4
Generator inertia about low speed shaft	kg-m^2	3.79×10^5	5.07×10^6
Turbine inertia about low speed shaft	kg-m^2	3.54×10^7	3.54×10^7
Equivalent drive-Shaft torsional-stiffness	Nm/rad	2.17×10^9	8.67×10^8
Equivalent drive-shaft torsional-damping constant	Nms/rad	2.85×10^6	6.21×10^6
Natural frequency in free–free mode for torsion (Hz)	Hz	12.1[a]	2.23[a]
Natural frequency in fixed–free mode for torsion (Hz)	Hz	1.24[a]	0.78[a]
Major equipment masses			
Power distribution equipment/cooling unit	ton	120	NA
Generator mass	ton	131	15.22
Shaft and housing	ton	28.5	NA
Turbine	ton	110	110
Brake disk, hydraulic system, yaw drive, nacelle frame	ton	50	NA

FWTDD: floating wind turbine with a direct-drive generator; NA: not available.
[a]Values computed based on NWTC recommendations.[39]

Table 4. Hub and nacelle properties.

Item/Description	Units	FWTDD system	NREL, 5MW baseline system[25,26]
Elevation of yaw bearing above ground	m	87.6	87.6
Vertical distance along yaw axis from yaw bearing to shaft centre	m	2.0	1.96
Distance along shaft from hub to yaw axis	m	4	5.01
Hub mass	kg	56,780	56,780
Hub inertia about low speed shaft	kg-m^2	115,926	115,926
Turbine mass	kg	53,233	53,233
Nacelle inertia about yaw axis	kg-m^2	2,115,474	2,607,890
Nacelle centre of mass from yaw axis	m	0.65[a] upwind	1.9 downwind
Nacelle CM location above yaw bearing	m	1.5[a]	1.75
Main bearing separation	m	2	NA
Shaft tilt angle	deg	5	5
Distance along shaft from hub centre to main bearing 1	m	0.65	NA
Distance along shaft from hub centre to main bearing 2	m	2.65	NA
Nominal nacelle-yaw rate	deg/s	0.3	0.3

[a]Initial estimates.
CM: centre of mass; FWTDD: floating wind turbine with a direct-drive generator; NA: not available.

Tower and platform properties

It was intended to achieve the same draft and ensure similar natural periods of rigid body motions as that of the geared FWT system[25] so that the global motion response characteristics for both systems were similar. At 330 tons, the direct-drive FWT nacelle was heavier than the geared system by 90 tons. Typically for every ton of extra mass at the nacelle, the tower mass increases by 2 tons. As a result the tower dimensions

Table 5. Resonance properties for different configurations.

Item	Units	Geared FWT system[25,48]	Designing for fatigue strength	Using denser ballast	Increasing spar length (draft)	Increasing spar diameter
Surge natural period	s	125	124.67	124.67	139.9	137.4
Heave natural period	s	31.4	31.62	31.62	35.39	34.92
Pitch natural period	s	29.1	47.87	35.37	44.8	37.48
Total platform mass including ballast	kg	7.46E + 06	7.13E + 06	7.13E + 06	9.27E + 06	11.02E + 06
Tower mass	kg	2.49E + 05	6.08E + 05	6.08E + 05	6.08E + 05	6.08E + 05

FWT: floating wind turbine.

for the original 5 MW turbine needed to be upgraded. It was intended to achieve the same fatigue life as that of the tower for a geared FWT. For this purpose, 22 short-term unidirectional responses from 4–25 m/s for the geared FWT were computed to determine the short-term fatigue life in turbulent wind field and irregular wave condition. The wind and wave climates were correlated by a method described by Johannessen et al.[42] Section 'Design load cases' provides the details of the wind and wave models. A wind probability distribution was then applied to calculate the long-term fatigue life for each of these 22 short-term responses. The same procedure was repeated for the FWTDD system resulting in a substantial increase in tower structural requirements, the overall inertia, the draft and altered the natural periods of the system. Column 3 in Table 5 shows the increase in tower mass and system natural periods, when attempting to match with the tower fatigue life as that of the geared system.

The ideal solution must ensure minimal change to platform design, mooring system design, system natural frequencies, motion response and the costs. Three options were investigated so as to support a heavier nacelle system with a direct-drive generator: using heavier ballast, increasing the length (and hence the draft) of the spar and increasing the spar diameter. It was observed that increasing the draft or spar diameter would bring major changes to the design and also add to a huge cost penalty. Increasing the spar draft increased the pitch stiffness and inertia. The tower height also had to be increased to see similar wind speed at the hub height. On the other hand, increasing the spar diameter increased the wave loads, altered the pitch stiffness and inertia and also required adjustments to the mooring design. While using a heavier ballast (for e.g., if steel is considered instead of gravel or water) can ensure minimal change to overall system design, it might prove to be expensive. Table 5 presents a comparison of properties with the spar length increased to 150 m and diameter increased by 1 m. Therefore, all of the above three options proved to be practically infeasible. The quickest approach to matching with the geared FWT system must seek to minimise the difference in nacelle mass to below 20 tons. The largest contributors to the heavy tower top mass for the FWTDD system include the generator, turbine, power transmission equipment. It was decided to retain the properties of the turbine to replicate the aerodynamic behaviour, therefore other options to reduce the nacelle mass were investigated for the FWTDD system.

Nacelle mass adjustments. With regards to generator mass, more structural solutions and alternative design topologies show significant weight-saving potential.[13,43–47] However, they introduce complexities (namely, manufacturing, dynamic balance for air gap). Therefore, it was decided not to disturb the generator topology. The next choice was relocating some mass from power conversion equipment to the tower bottom. This can help eliminate the need to install a transformer and heavy low voltage cables, and relocate critical equipment to the bottom of the tower where vibrations generated by the platform motion is considerably lower. This resulted in a nacelle mass of 255 tons, which was comparable with the geared system (240 tons). The resulting platform hydrostatic and resonance properties of the FWTDD system are summarised in Table 6. Figure 4 shows the location of the nacelle CM after the mass adjustment.

Tower structural properties. The main dimensions of the tower were not altered, but in order to account for additional 15 tons at the nacelle and to match the fatigue life of the baseline system the tower thickness was adjusted by about 9%. This increased the overall tower mass by 128 tons against the baseline system.[25] The tower was assumed to be linearly tapered with thickness at base and top levels at 0.0381 m and 0.027 m, respectively. Tables 7 and 8 give the distributed and un-distributed tower structural properties. The entries in Table 7 refer to the tower section-wise data for mass density, stiffness, inertia and mass offsets in the fore-aft and side-to-side directions with terminologies as defined in Jonkman and Buhl.[49]

Platform structural properties. The main dimensions of the platform, including the tapered conical section

Table 6. Spar properties.

Item/Description	Units	FWTDD system	NREL, 5 MW baseline system[4,48]
Nacelle centre of mass from yaw axis	m	2.5 upwind	1.9 downwind
Nacelle CM location above yaw bearing	m	1.9	1.75
Centre of gravity of the entire system	m	−77.56	−78.61
Surge/sway natural period	s	125.6	125
Heave natural period	s	31.4	31.4
Roll/pitch natural period	s	29.9	29.1
Yaw natural period	s	7.57	5

CM: centre of mass; FWTDD: floating wind turbine with a direct-drive generator.

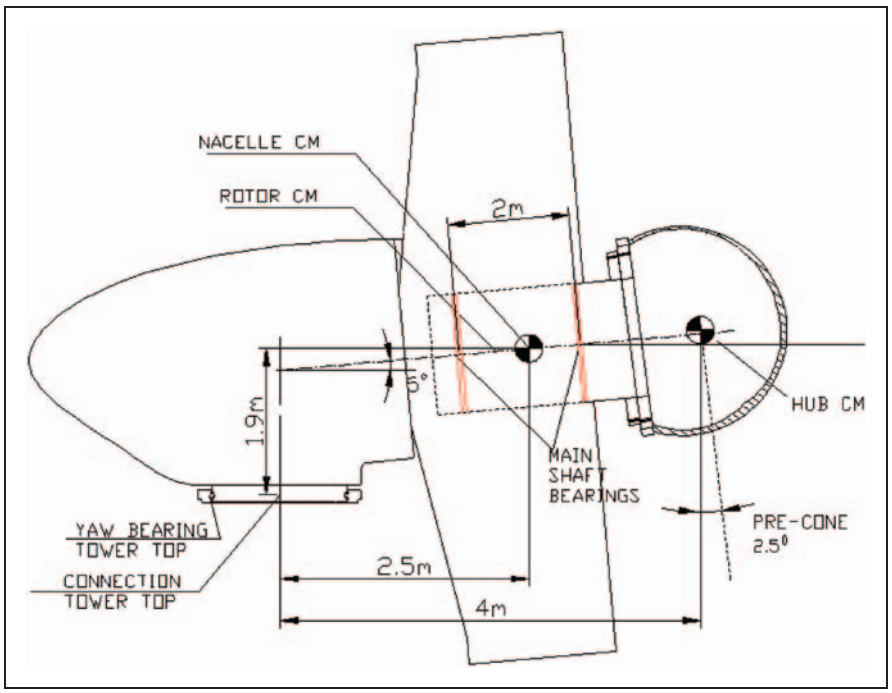

Figure 4. Nacelle CM after mass adjustments.

Table 7. Distributed tower properties.

HtFract	TMassDen	TwFAStif	TwSSStif	TwGJStif	TwEAStif	TwFAIner	TwSSIner	TwFAcgOf	TwSScgOf
(–)	(kg/m)	(Nm^2)	(Nm^2)	(Nm^2)	(N)	(kg-m)	(kg-m)	(m)	(m)
0	6104.43	6.65E + 11	6.65E + 11	5.12E + 11	1.50E + 11	27,469.9	27,469.9	0	0
0.1	5713.10	5.79E + 11	5.79E + 11	4.46E + 11	1.41E + 11	23,916.0	23,916.0	0	0
0.2	5334.62	5.02E + 11	5.02E + 11	3.86E + 11	1.31E + 11	20,718.0	20,718.0	0	0
0.3	4969.00	4.32E + 11	4.32E + 11	3.32E + 11	1.22E + 11	17,851.3	17,851.3	0	0
0.4	4616.24	3.70E + 11	3.70E + 11	2.85E + 11	1.14E + 11	15,292.4	15,292.4	0	0
0.5	4276.32	3.15E + 11	3.15E + 11	2.42E + 11	1.05E + 11	13,018.3	13,018.3	0	0
0.6	3949.27	2.66E + 11	2.66E + 11	2.05E + 11	9.75E + 10	11,007.2	11,007.2	0	0
0.7	3635.06	2.23E + 11	2.23E + 11	1.72E + 11	8.98E + 10	9238.1	9238.1	0	0
0.8	3333.72	1.86E + 11	1.86E + 11	1.43E + 11	8.23E + 10	7690.7	7690.7	0	0
0.9	3045.22	1.53E + 11	1.53E + 11	1.18E + 11	7.52E + 10	6345.8	6345.8	0	0
1.0	2769.58	1.25E + 11	1.25E + 11	9.65E + 10	6.84E + 10	5185.0	5185.0	0	0

Table 8. Undistributed tower properties.

Item/Description	Units	FWTDD system	5 MW spar system[4]	NREL, 5 MW baseline system[25]
Elevation to tower base (platform top) above SWL	m	10	10	10
Elevation to tower top (yaw bearing) above SWL	m	87.6	87.6	87.6
Overall (integrated) tower mass	kg	377,564	347,460	249,718
CM location of tower above SWL along tower centreline	m	38.36	NA	43.4
Tower structural damping ratio (all modes)	%	1	1	1

CM: centre of mass; SWL: sea water level; FWTDD: floating wind turbine with a direct-drive generator; NA: not available.

Table 9. Platform structural properties.

Item/Description	Units	FWTDD system	NREL, 5 MW baseline system[25]
Depth to platform base below SWL (total draft)	m	120	120
Elevation to platform top (tower base) above SWL	m	10	10
Depth to top of taper below SWL	m	4	4
Depth to bottom of taper below SWL	m	12	12
Platform diameter above taper	m	6.5	6.5
Platform diameter below taper	m	9.4	9.4
Platform mass, including ballast	kg	7,365,000	7,466,330
CM location below SWL along platform centreline	m	93.21	89.91
Platform roll/pitch inertia about CM	kg-m^2	7.33×10^{10}	4.22×10^9
Platform yaw inertia about platform centreline	kg-m^2	1.03×10^8	1.64×10^8

CM: centre of mass; SWL: sea water level; FWTDD: floating wind turbine with a direct-drive generator.

remain the same as that of the baseline system. The draft was maintained at 120 m. The mass of the platform including ballast was 7365 tons. The CM of the floating platform, including ballast, is located 93.2 m along the platform centreline below the SWL. Table 9 presents the platform properties for the FWTDD system with the values for the baseline system provided for reference.

Mooring properties

The layout and properties of the mooring system were retained from Karimirad and Moan.[4] Three sets of mooring lines with fairleads located on the circumference of the spar form a delta configuration. The mooring system characteristics namely the diameter, length and masses of the mooring segments were found to be sufficient for the FWTDD system, hence no modifications were required. The line stiffness and pretensions were consistent with Karimirad and Moan.[4] Table 10 summarises the mooring system properties and Figure 5 shows the schematic layout for the FWTDD system with mooring lines.

The overall mass of the FWTDD system including mooring lines was computed as 8396 tons, although further attempts on optimisation can result in further reduction in the weights. As may be noted from Figure 6, this compares well with some of the other spar designs that have been under research.

Table 10. Mooring system properties.

Item/Description	Units	FWTDD system
Number of Mooring lines	–	3
Angle between adjacent lines	deg	120
Depth to anchors below SWL (water depth)	m	320
Depth to fairleads below SWL	m	70.0
Radius to anchors from platform centreline	m	853
Radius to fairleads from platform centreline	m	5.2
Un-stretched Mooring line length	m	902.2
Mooring line diameter	m	0.09
Clump mass	kg	17,253
Equivalent Mooring line mass density	kg/m	42.5
Equivalent Mooring line weight in water	N/m	381.8

SWL: sea water level; FWTDD: floating wind turbine with a direct-drive generator.

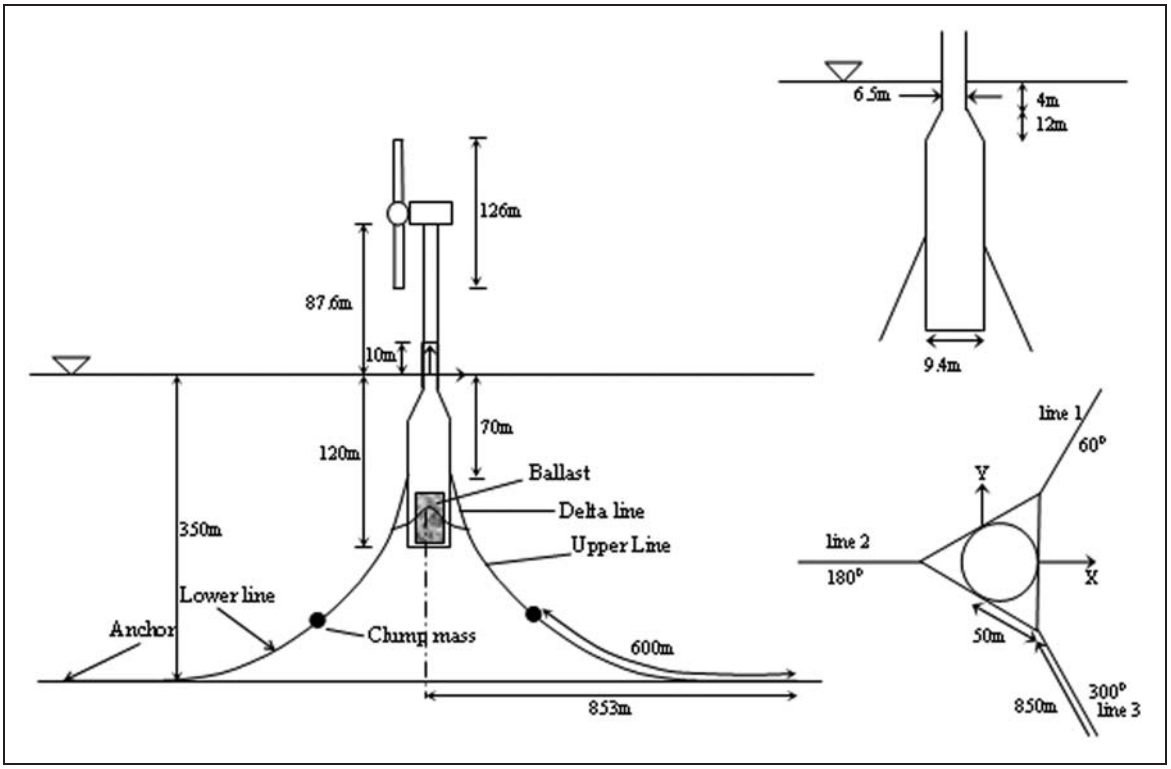

Figure 5. Mooring layout for the FWTDD system.

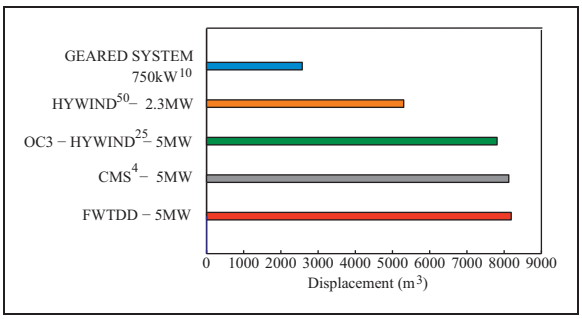

Figure 6. A comparison of FWTDD system with existing spar designs.
FWTDD: floating wind turbine with a direct-drive generator.

Wind turbine controller properties

The NREL 5 MW wind turbine is described by quasi-static rotor model for controlling the aerodynamic efficiency. Variable speed operation of the wind turbine with power regulation can be achieved with direct-drive wind generators either by active blade-pitch control or stall control.[51] The conventional variable blade-pitch control system was chosen and implemented using controllers for generator torque and blade-pitch angle. The generator speed is the measured variable that is filtered using a recursive low-pass filter before being fed as input to the controllers. The demand torque from the generator is established by a proportional–integral (PI) velocity controller. The matching between the aerodynamic torque and the electromechanical torque of the generator determines the reference pitch angle rotor speed.

Table 11. Control laws.

Region 1	0
Region 1½	$(1.063\Omega - 7.33) \times 10^6$
Region 2	$\left(\frac{\pi}{30}\right)^2 K_T \Omega^2$
Region 2½	$(2.107\Omega - 20.6) \times 10^6$
Region 3	1.1 T_{rated}

Generator-torque control

Since the direct-drive generator is characterised by a high torque operation at lower speed, this implies different dynamics for the control action and hence requires adjustments to the control parameters originally defined for the geared system in Jonkman.[25] The wind turbine is operated according to five different control laws as listed in Table 11 depending on the measured generator speed.

As may be noted from Figure 7, the turbine start-up occurs in region 1, for generator-speeds between 0 and 6.9 r/min. Once the generator speed has accelerated to 6.9 r/min, the generator torque is switched ON and power is produced normally. The region 2 torque curve is intended to keep the turbine operating at the peak of its C_p–λ curve and follows the square law defined in Table 11, where Ω is the filtered generator

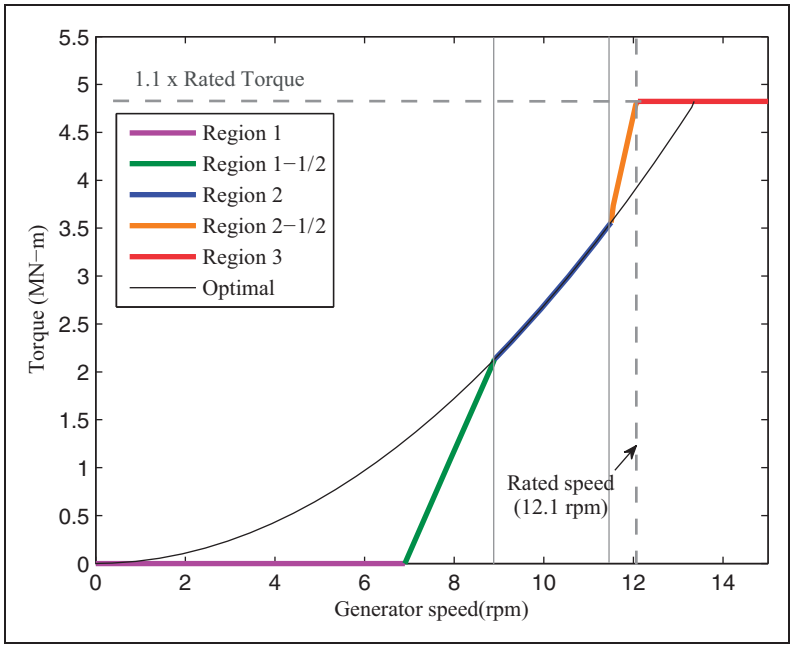

Figure 7. Generator speed–torque characteristics.

speed (r/min), k_T is the nominal optimum torque control gain (Nms^2/rad^2) given by

$$k_T = \frac{1}{2}\rho\pi R^5 \frac{C_{p\max}}{\lambda_*^3} \approx \frac{P_{rated}}{\Omega_0^3} \quad (1)$$

where R is the rotor radius, $C_{p\max}$ is the maximum power co-efficient, λ_* is the tip-speed ratio at $C_{p\max}$ and P_{rated} is the rated mechanical power of the turbine. To account for turbulence in wind speeds, maximise energy capture and reduce the loads on the drive-train, the torque gain is set to about 90% of the optimum.[52] For a rated speed of 12.1 r/min (i.e. 1.2679 rad/s), equation (1) gave a value of 2.45 MN-ms^2/rad^2 for the torque gain that was higher than the baseline system by a factor of about 10^6. Region 1½ is a linear transition in the start-up region that spans the range of generator speeds between 6.9 r/min and 30% above this value (or 8.9 r/min). Figure 7 shows the optimal torque curve (region 2 control law) crossing the rated torque line at a higher rotor speed than the rated speed (i.e. 12.1 r/min). In order for the generator torque to be equal to rated torque at rated speed, a new region 2½ is introduced[53] such that the torque is described using the equation as listed in Table 11.

In region 3, for above-rated wind speed, the control switches to a constant torque mode with active pitch control to avoid negative aerodynamic damping as per Larsen and Hanson[54] and Larsen.[55] The generator torque in region 3 is set to be saturated to a maximum of 10% of the rated torque to avoid excessive overloading of the generator.

Since the electrical system was not modelled, the generator torque is assumed to instantly follow the controller set-point assuming a faster dynamic response from electrical system. However, because of a very low inertia of the generator rotor, a quick response is particularly important during start-up and when operating above the rated wind speed. For this purpose, the maximum generator torque rate was imposed at 1×10^8 Nm/s.

Blade-pitch controller

The blade-pitch control system is designed to be effectual on the torsional degree of freedom of the drive-train for the above-rated wind speeds. The servo system is implemented by a PI controller that provides a reference pitch angle depending on the measured generator speed. Above-rated wind speeds, the aerodynamic torque T_{Aero} was linearised assuming negligible variation in rotor speed and greater sensitivity to pitch angle, θ. The blade-pitch angle is regulated by measuring the generator speed error using PI controller.[54] A gain-scheduling law was implemented to predetermine the set of controller tuning parameters. The values for the controller gains were determined assuming a second order response system (as defined in Larsen and Hanson[54]) with natural response frequency, ω_0, relative damping ζ and damped natural frequency ω_d, such that

$$\omega_0 = \frac{\omega_d}{\sqrt{1-\zeta^2}} \quad (2)$$

To eliminate servo-induced instability and negative aerodynamic damping, the gains were tuned such that $\omega_d < \omega_{pitch}$ (the pitch natural frequency).[54,55] The natural frequency of the controller (0.0142 Hz) was set to

Table 12. Controller properties.

Item/Description	Units	FWTDD system	NREL, 5 MW baseline system[25]
Corner frequency of generator-speed low pass filter	Hz	0.25	0.25
Peak power coefficient	–	0.482	0.482
Tip speed ratio at C_{pmax}	–	7.55	7.55
Rotor-collective blade-pitch angle at peak power Coefficient	deg	0	0
Generator-torque constant in region 2	Nms^2/rad^2	2,455,061.04	2.332
Generated rated power	MW	5.56	5.29
Rated generator torque	MN-m	4.38	0.043
Generator speed between 1 and 1½	r/min (rad/s)	6.9 (0.722)	670 (70.16)
Transitional generator speed between regions 1½ and 2	r/min (rad/s)	8.9 (0.932)	871 (91.21)
Transitional generator speed between regions 2½ and 3	r/min (rad/s)	11.9 (1.246)	1161.9 (121.67)
Minimum blade-pitch for ensuring region 3 torque	deg	1	1
Maximum generator torque	MN-m	4.8	0.047
Maximum generator torque rate	MN-m/s	100	0.015
Proportional gain at minimum blade-pitch setting	s	2.11	0.006275
Integral gain at minimum blade-pitch setting	–	0.094	0.000896
Blade-pitch angle at which the rotor power has doubled	deg	6.302	6.302
Minimum blade-pitch setting	deg	0	0
Maximum blade-pitch setting	deg	90	90
Maximum absolute blade-pitch rate	deg/s	8	8

FWTDD: floating wind turbine with a direct-drive generator.

be lower than the pitch natural frequency (0.033 Hz) of the FWTDD system so that the blade-pitch control is slower than the tower motion. This value was chosen after verifying the controller stability in different wind conditions. Section 'Controller stability' provides a discussion on controller performance and stability. The resulting properties of the controller are summarised in Table 12.

Modelling and response analysis of the FWTDD system using HAWC2

A fully coupled aero-hydro-servo elastic model of the FWTDD system was implemented in HAWC2[14] for the specifications that were developed in this study. HAWC2 is an aero-elastic simulation code developed by Risø National Laboratory that can simulate the time domain response of a wind turbine subjected to wind, wave and control system actions. The code is based on a multi-body formulation which uses the classic Timoshenko beam element considering FEA for the structural dynamics and an advanced blade element momentum theory for the aerodynamics. The various elements namely the tower, foundation, shaft/nacelle and rotor for the FWTDD system were modelled and assembled together by geometric sub-structuring technique. The turbine and nacelle were modelled as rotating substructures coupled to each other and the tower.

The aerodynamic loads are derived from quasi-static theory with mean wind field effects including correction factors for induction; tip-loss, shear, tower drag, shadow effects (based on potential flow method) and turbulence generated according to Mann method.[56] Turbulence intensity was defined according to Class C (for offshore wind turbines). Wind turbine blades are modelled as long and slender structures with wind flow at a given point assumed to be two dimensional.

Wave kinematics at every time step uses airy wave theory, with wheeler stretching and the hydrodynamic forces are calculated from the instantaneous position of every strip of the floater using the Morison equation considering relative velocity formulation.[57] An added mass coefficient of 1.0 and a drag coefficient of 0.6 were assumed. Since the Morison formula does not provide heave excitation and buoyancy forces, HAWC2 uses Archimedes plus static pressure integration methods over the bottom and conical sections of the spar to calculate the vertical forces.[58]

Mooring lines use a simplified quasi-static force model implemented as DLLs. 1 DOF torsional spring-damper system was implemented for the drive-train with the flexible elements modelled as shaft elements with mass, structural stiffness and damping properties. The generator is modelled as a separate rotational degree of freedom with the speed–torque characteristics modelled as a force element DLL. HAWC2 solves the equations of motion by a time integration scheme and presents the results as time series for loads and deformations. The following sub-section describes the design load cases that were considered for this study.

Design load cases

To begin with, the consistency and performance of the FWTDD system was verified for normal power production as defined in IEC-61400-3.[59] For this purpose, turbulent wind field and irregular wave condition were considered. Wave and wind data were correlated for a representative site (Statfjord in North Sea) from site measurements using the analytical models described by Johannessen et al.[42] These models relate the expected values of significant wave height and peak wave periods to a given average wind speed at hub height. The 1-hour mean wind speed distribution at 10-m height, was defined by a two-parameter Weibull distribution expressed as

$$F(V) = 1 - \exp[-(V/\beta)^{\alpha}] \tag{3}$$

where V (m/s) is the mean 10-min wind speed at 10 m with shape and scale parameters $\alpha = 1.708$ and $\beta = 8.426$. The average wind speed at hub-height was then obtained by scaling the wind speed at 10 m height using the power law with a power co-efficient of 0.14. To obtain the 10-min average wind speeds, 10% scaling was applied to 1-hour average wind speeds. The turbine cuts in at 4 m/s and cuts out for wind speed above 25 m/s. The expected values of significant wave height, $E(H_{m0})$ and peak wave period, $E(T_p)$ were obtained from the mean 10-min wind speed, V (m/s) using the following equations[42] to define long-crested irregular waves represented by JONSWAP wave spectrum[60]

$$E(H_{m0}) = \beta\Gamma\left(\frac{1}{\alpha} + 1\right) \tag{4}$$

where $\alpha = 2 + 0.135\,V$ and $\beta = 1.8 + 0.1\,V^{1.322}$ and

$$E(T_p) = \left(4.883 + 2.68H_{m0}^{0.529}\right) \times \left(1 - 0.19\frac{V - (1.764 + 3.426H_{m0}^{0.78})}{(1.764 + 3.426H_{m0}^{0.78})}\right) \tag{5}$$

Blade-pitch angle equals zero below rated and 90° at cut-out. Twenty-two unidirectional wind and wave load cases spanning the turbine operational region, i.e. 4–25 m/s, were considered as listed in Table 13.

Table 13. Design load cases.

Load case	V_{mean}	H_{m0}	ω_p $(2\pi/T_p)$	$\lambda = \frac{gT_z^2}{2\pi}$
–	(m/s)	(m)	(rad/s)	(m)
1	4	1.96	0.646	89.29
2	5	2.08	0.645	89.56
3	6	2.22	0.643	90.12
4	7	2.36	0.641	90.69
5	8	2.52	0.638	91.54
6	9	2.68	0.634	92.70
7	10	2.84	0.630	93.88
8	11	3.01	0.626	95.08
9	12	3.19	0.622	96.31
10	13	3.37	0.617	97.88
11	14	3.55	0.612	99.48
12	15	3.75	0.607	101.13
13	16	3.94	0.602	102.82
14	17	4.14	0.597	104.55
15	18	4.35	0.591	106.68
16	19	4.55	0.586	108.51
17	20	4.77	0.581	110.38
18	21	4.98	0.576	112.31
19	22	5.20	0.570	114.69
20	23	5.43	0.565	116.72
21	24	5.65	0.560	118.82
22	25	5.88	0.555	120.97

V_{mean}: 10-min mean wind speed at hub height; H_{m0}: significant wave height; ω_p: the peak wave frequency; λ: the wavelength; T_z: zero up-crossing period ($T_z = T_p/1.2859$ for JONSWAP spectrum[61]).

Controller stability

Controller tuning and stability are important aspects that need to be evaluated carefully for a FWT system.[54] The specifications of the controller properties defined in section 'Wind Turbine Controller properties' were incorporated into control system dynamic link library (DLL) in HAWC2 model. In order to evaluate the performance and stability of the controller, time response simulations were carried out where the turbine was subjected to deterministic wind speeds as recommended by Larsen and Hanson.[54] The stability of the control system was first tested by observing the spar response to a linearly increasing wind velocity up to 16 m/s. No waves were assumed to be present. Figure 8(a) to (d) shows the simulation results for shaft speed, blade-pitch action and platform surge motion. Rotor speed overshoots by 7% of the rated (i.e. 12.1 r/min) to about 13 r/min at 300 s while the platform surges up to a maximum of 22 m between 150 s and 300 s during which the wind ramp up occurs. It takes about 700 s for the surge response to stabilise.

The controller performance was further tested in step winds. Both floating as well as land-based direct-drive wind turbine system (WTDD) were tested with the same controller. For the WTDD system, the foundation and mooring lines were removed and the tower was cantilevered to the soil floor.

Figure 9(a) to (e) shows the simulation results for shaft speed, generator torque, blade-pitch angle and platform surge motion for step wind condition from 11 m/s to 13 m/s. The controller response frequency was initially kept at 0.125 rad/s (or 50 s). However, considerable blade-pitch instability was observed after 700 s of simulation causing fluctuations in

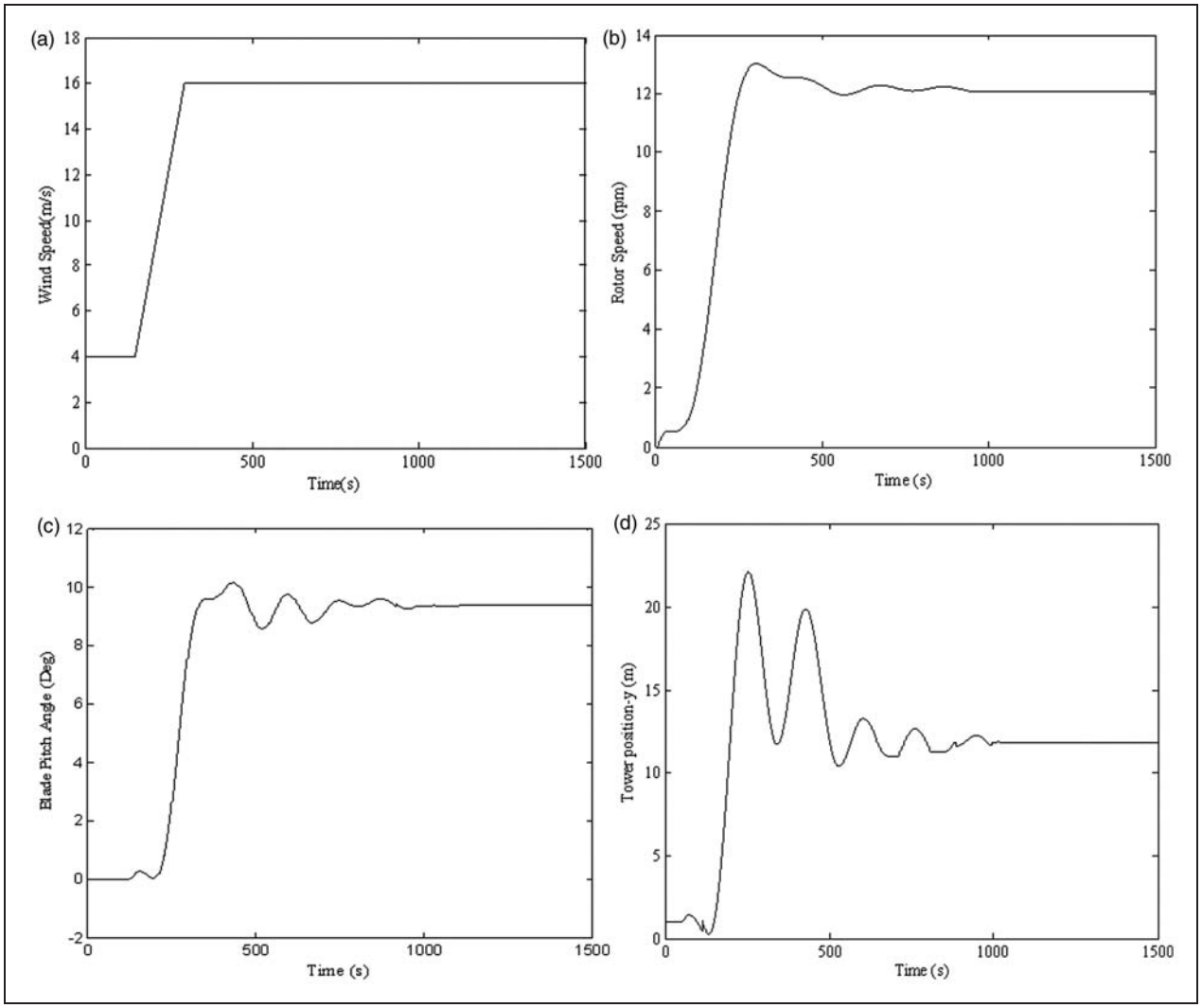

Figure 8. Tower motion response and controller response for a deterministic wind speed: (a) wind speed; (b) rotor speed; (c) blade pitch angle; (d) tower position.

generator torque and speed response. To ameliorate this problem, the controller response frequency was suitably adjusted until a more stable response was achieved for the given wind conditions. The controller response frequency was progressively reduced from 0.125 rad/s until 0.09 rad/s (or 70 s) when a more stable response was achieved. Figure 10(a) to (e) shows the response for the adjusted system. A better overall performance is seen with overshoot in rotational speed below 10% for the land-based wind turbine and 16% for the floating system. Moderate spikes are observed in the blade-pitch response every time wind ramps up for the WTDD system. The oscillation in blade-pitch response and shaft speed for the FWTDD system is induced by platform motions (particularly by pitch motion). This also explains for the oscillatory response in torque after 600 s for the FWTDD system while the platform surges up to a maximum of 47 m. The tower response for the WTDD system is provided for reference in Figure 10(e). Thus, the properties for the controller were found to ensure a stable response for the given wind conditions, although the controller response was not optimised for all operating conditions.

Global motion response

Twenty-two 1-hour simulations were carried out by subjecting the HAWC2 model to a combination of unidirectional wind (4–25 m/s) and wave loads (2–6 m wave heights) as defined in Table 13 and the motion responses were extracted. A comparison was made with the 5 MW geared FWT system that was modelled in HAWC2 using the specifications presented in Jonkman.[25] The results for nacelle motion response statistics (Figure 11) show a steady increase in surge and pitch responses up to 11 m/s beyond which the responses begin to smoothen out. The maximum pitch angle predicted with both the systems was less than 8°. It can be inferred from the response characteristics that the behaviour of the FWTDD system closely resembled that of the geared FWT system. Since, 1-hour simulations were considered, statistical uncertainty may be present for the below-rated and

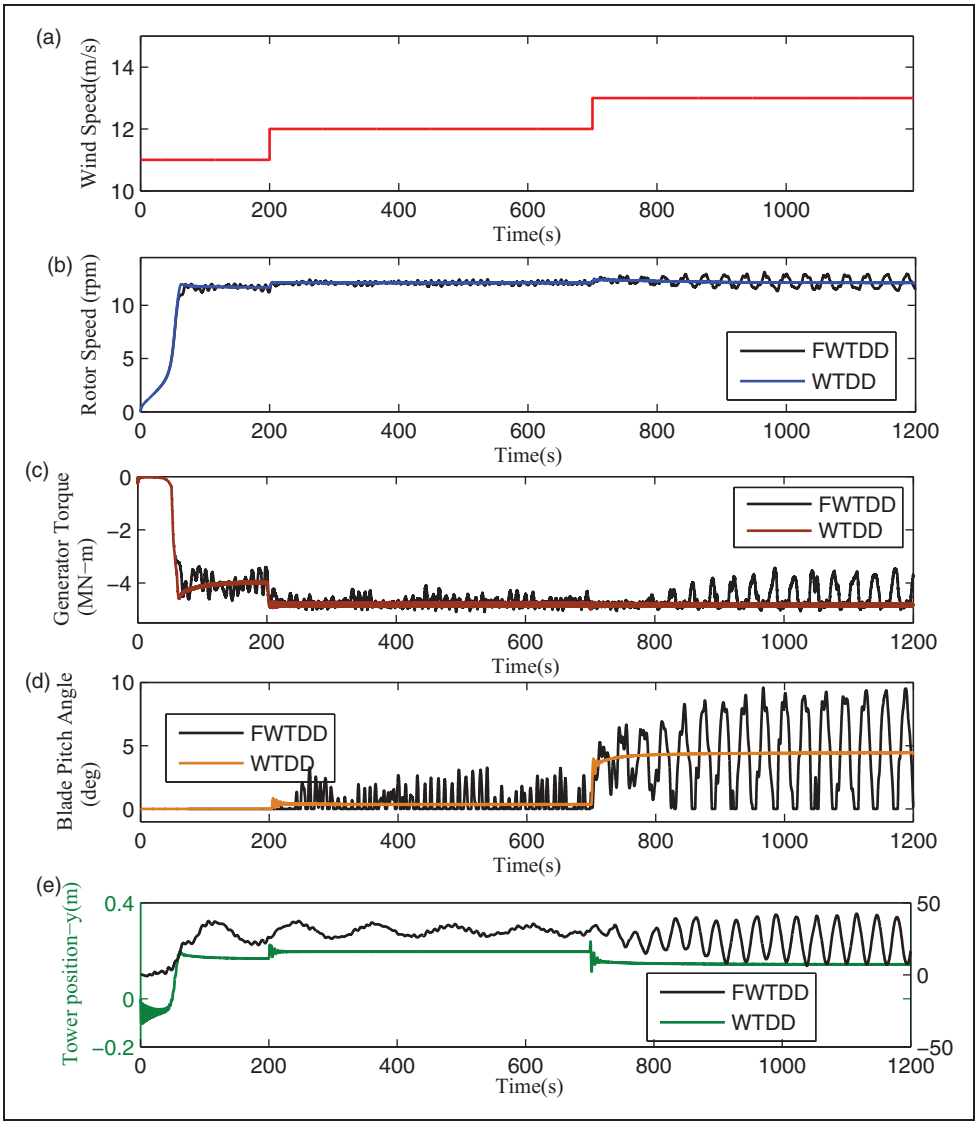

Figure 9. Step response: (a) wind speed; (b) shaft rotational speed; (c) generator torque; (d) blade-pitch angle; (e) tower position. FWTDD: floating wind turbine with a direct-drive generator; WTDD: Land-based wind turbine with a direct-drive generator.

above-rated wind speed conditions. Nevertheless, the preliminary results show that the motion response was generally consistent with the typical response characteristics observed for the spar buoy wind turbine.[4]

Aerodynamic response and main shaft loads

The aerodynamic responses of the geared and direct-drive FWT systems were compared and the results are presented in Figures 12 and 13. As may be observed from Figure 12, the FWTDD system experiences a greater mean aerodynamic thrust above-rated wind speeds when compared to the geared FWT system. This difference also manifests on the aerodynamic rotor power curves plotted for the mean values for the two systems (Figure 13). In region 3 (refer to Figure 7), as was pre-defined by generator efficiency in the controller reference settings, the mean values for the rotor power settles at around 5.56 MW and 5.29 MW for the FWTDD and geared FWT system, respectively. The average values of the shaft speed above rated wind speed in region 3 was around 12.12 r/min and 12.14 r/min respectively for the geared and direct-drive systems (Figure 14).

Apart from the motion response characteristics and aerodynamic loads, HAWC2 also provides information on main shaft moments and forces. For a given wind and wave condition, it is reasonable to assume the short-term load response as a stationary random process. The analysis of such processes require statistical treatment of the time histories for the response variables obtained through numerical simulations. The mean, standard deviation and maximum values of measured variables provide some useful information on the loading of drive-train components for determining the adequacy of the design, component strength and predicting their lifetime. Since the dynamics of the direct-drive system is bound to differ greatly from the geared system, it would be more meaningful to make a comparison of

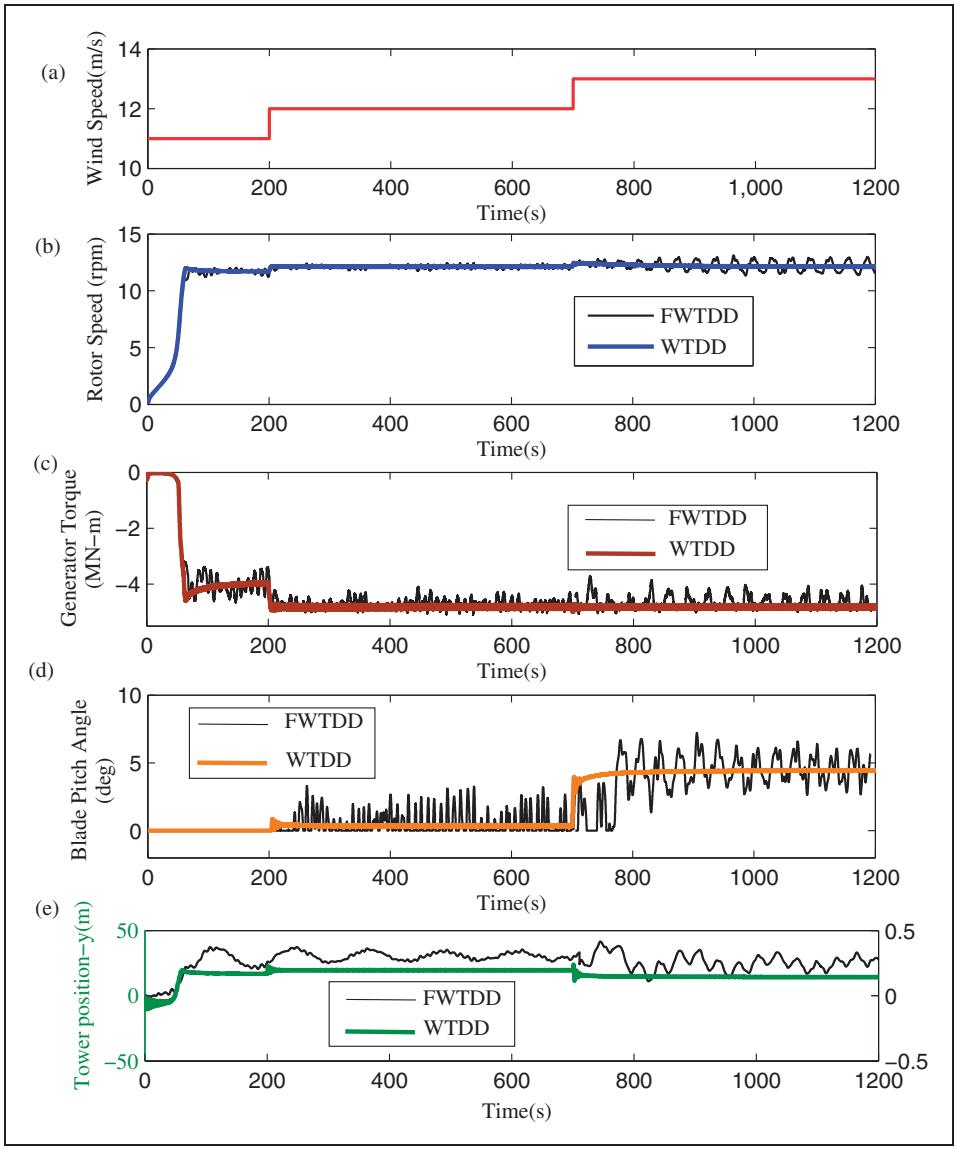

Figure 10. Step response-adjusted: (a) wind speed (b) shaft rotational speed; (c) generator torque; (d) blade-pitch angle; (e) tower position.
FWTDD: floating wind turbine with a direct-drive generator; WTDD: Land-based wind turbine with a direct-drive generator.

the main shaft loads for the land-based and floating versions direct-drive wind turbine systems inorder to make logical inferences on the performance. A comparison of the main shaft loads predicted by HAWC2 simulations (subsequent section) showed only a marginal increase for the FWTDD system which is a favourable attribute.

Comparison of main shaft loads. Figure 15 presents a comparison of the main shaft load statistics for the normal operating range of the wind turbine (4–25 m/s) for the floating and land-based versions of the direct-drive system. The load components compared include torque, axial force, resultant shear force (the sum contribution of forces in the in-plane direction) and bending moments (the sum contribution of moments in the in-plane direction). The values are expressed as a percentage difference of FWTDD response with the land based counterpart as

$$\%difference = \frac{X_{FWTDD} - X_{WTDD}}{X_{WTDD}} \times 100\% \qquad (6)$$

where X_{WTDD} is the response variable measured from the land-based model and X_{FWTDD} is the corresponding value for the offshore floating model.

Figure 15(a) to (c) shows that there is only a marginal variation of the mean, standard deviation and maximum values of bending moments and torques for the FWTDD system. The values for bending moments for FWTDD system are lower for wind speeds below rated, yet the difference is negligible with up to 3.5%, 2.5% and 1.79% respectively for mean, standard deviation and maximum values. Similar trend is noted for

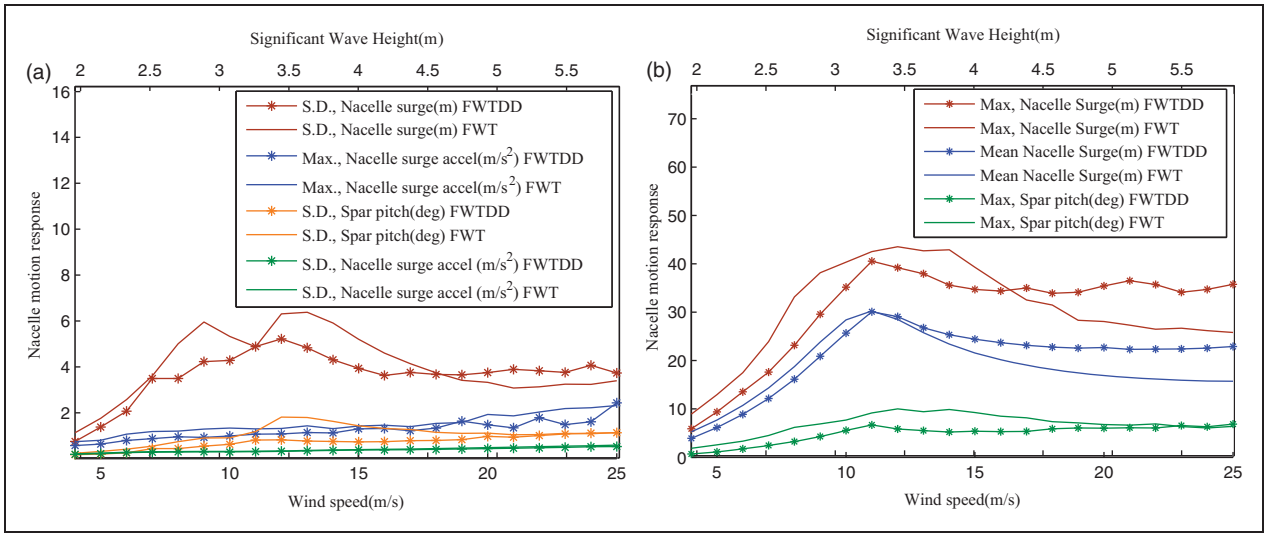

Figure 11. Nacelle motion response statistics from HAWC2 simulations for FWTDD and FWT systems.
FWTDD: floating wind turbine with a direct-drive generator; FWT: floating wind turbine (geared).

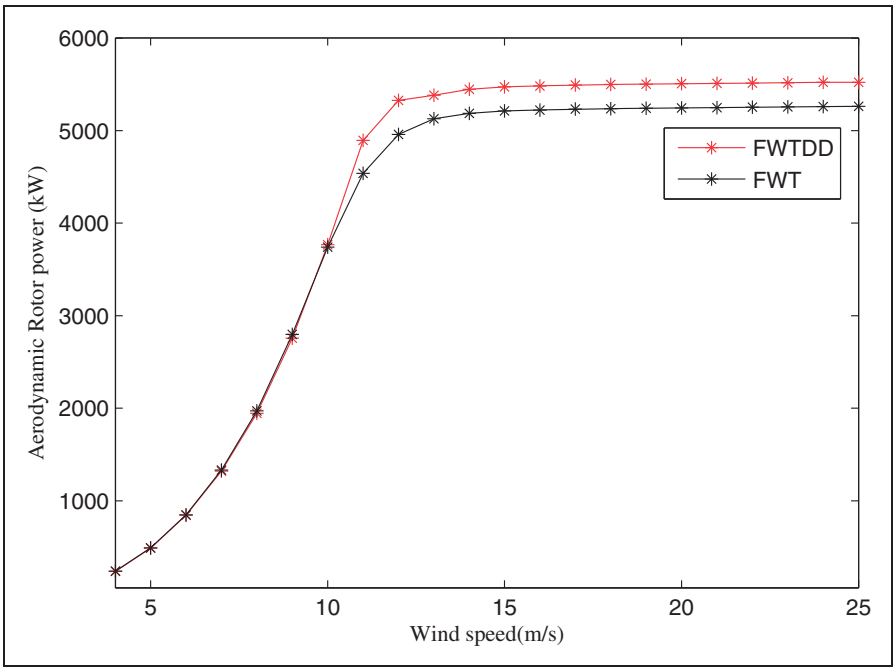

Figure 12. Aerodynamic rotor power curves for FWTDD and FWT systems.
FWTDD: floating wind turbine with a direct-drive generator; FWT: floating wind turbine (geared).

torque values below rated wind speeds with less than 3% difference in standard deviation values. The difference in mean values for the axial forces tends to increase up to 12 m/s wind speed and settles close to about 10% for wind speeds above rated (i.e. 12 m/s).

The mean values for shear forces are lower in the case of FWTDD, with less than 1% difference in the maximum values. Yet, the data points for shear forces for the FWTDD were found to be widely dispersed at wind speeds below rated leading to more than 100% difference in standard deviation. This is also because the absolute values of the standard deviations for shear forces were small. These values range from 2.46 kN to 57.8 kN for WTDD and 5.3 kN to 61.3 kN for FWTDD system. The same can be deduced for the standard deviations in axial forces that vary from 20 kN to 115 kN for the WTDD system and 20 kN to 99 kN for the FWTDD system. The maximum values of the main shaft loads for the FWTDD are within 12% as compared to the WTDD

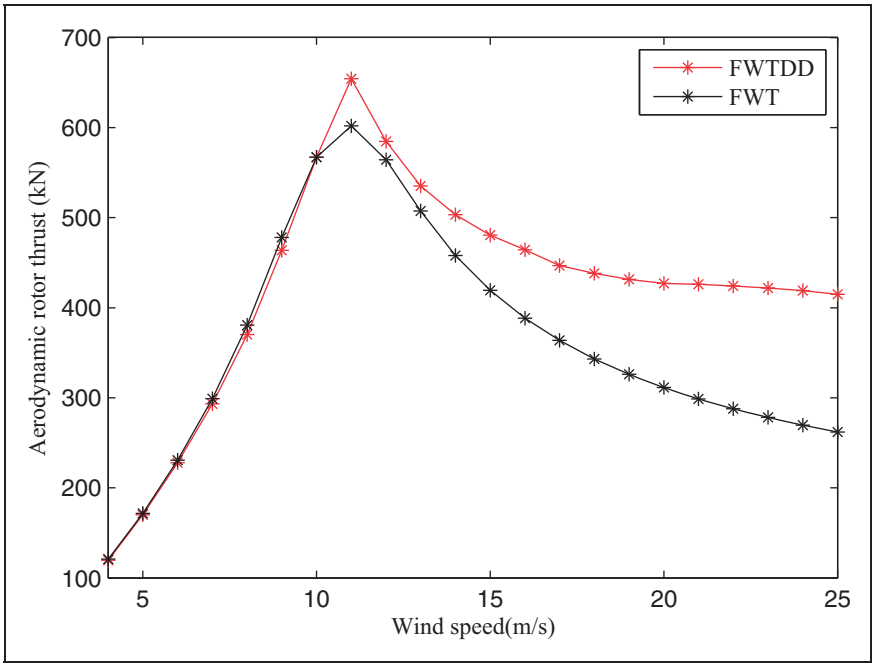

Figure 13. Aerodynamic rotor thrust for FWTDD and FWT systems.
FWTDD: floating wind turbine with a direct-drive generator; FWT: floating wind turbine (geared).

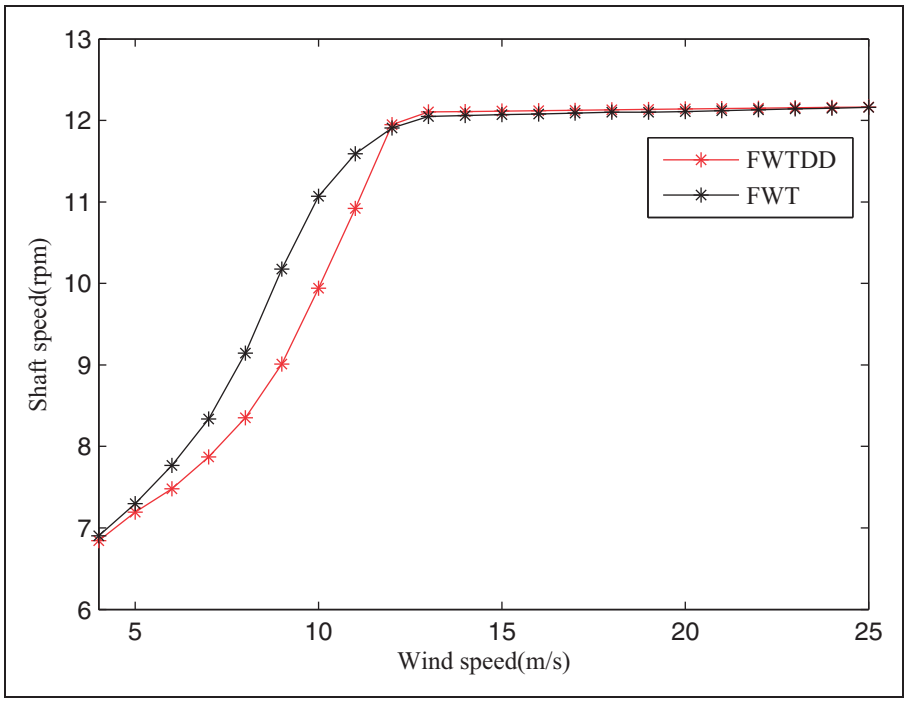

Figure 14. Shaft speed response for FWTDD and FWT systems.
FWTDD: floating wind turbine with a direct-drive generator; FWT: floating wind turbine (geared).

system with the exception of axial loads. The maximum axial loads tend to increase at an average of 24% for the FWTDD system.

The power spectral densities for the main shaft loads at 20 m/s wind speed (Figures 16 to 19) show the additional sources of excitation for the FWTDD system. Apart from a couple of very low frequency excitations, the load spectra for the main shaft shear force for the FWTDD system show additional response peaks associated with the wave excitation frequency, platform's pitch natural frequency and slightly higher excitation due to rotor 2P, 3P and

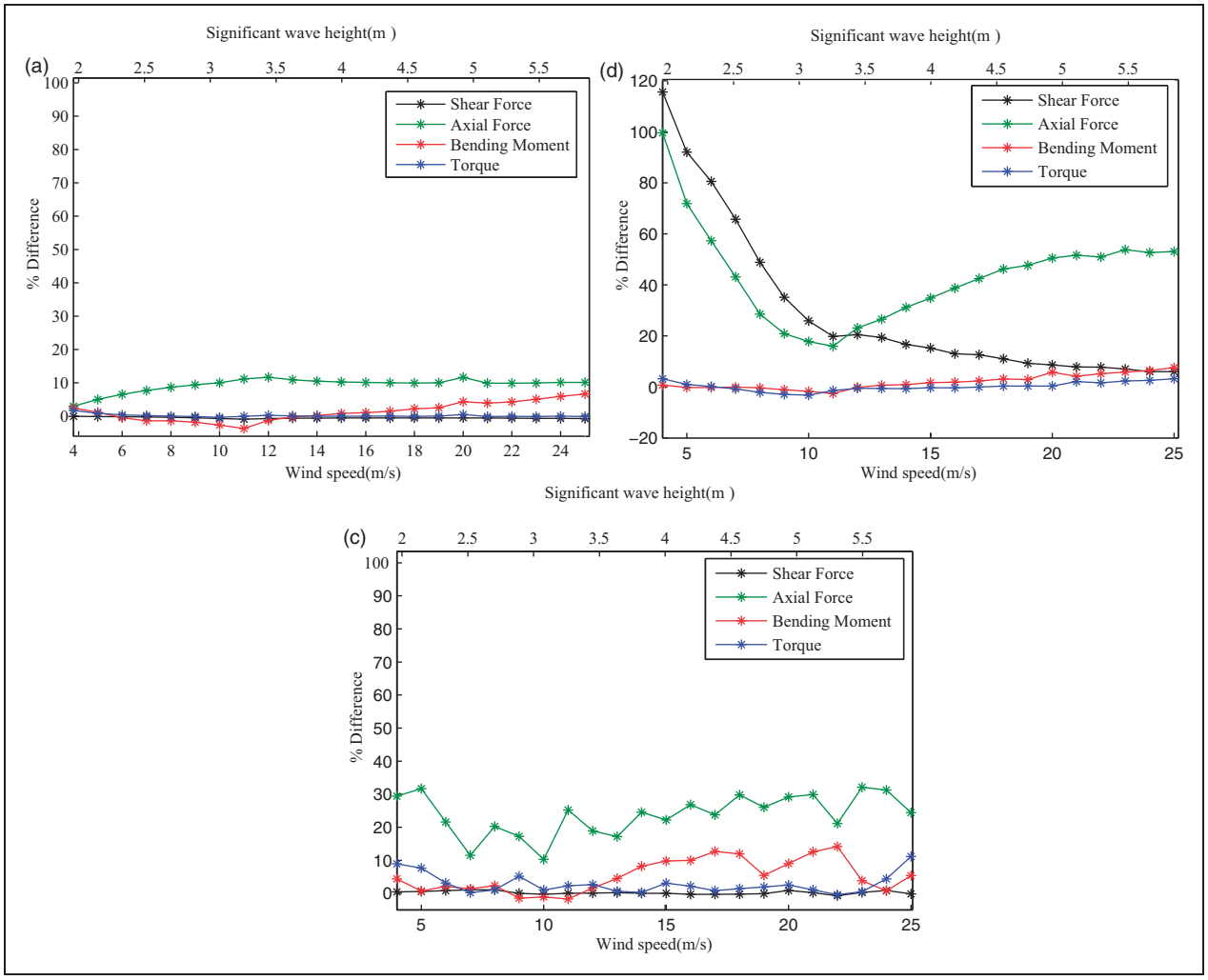

Figure 15. % Difference in main shaft loads – FWTDD vs WTDD systems (a) Mean values; (b) Standard deviation; (c) Maximum values.

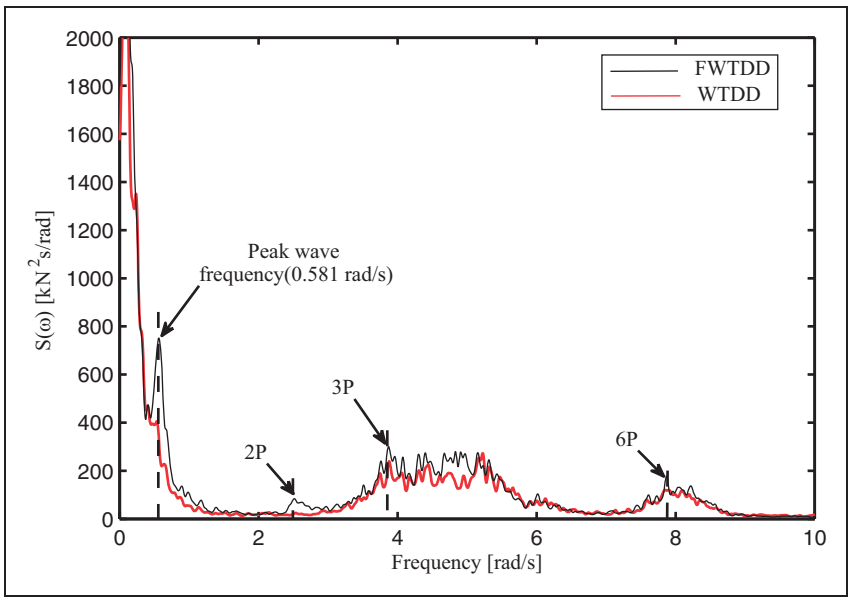

Figure 16. Frequency spectra of main shaft shear forces – FWTDD vs WTDD systems.
FWTDD: floating wind turbine with a direct-drive generator; WTDD: Land-based wind turbine with a direct-drive generator.

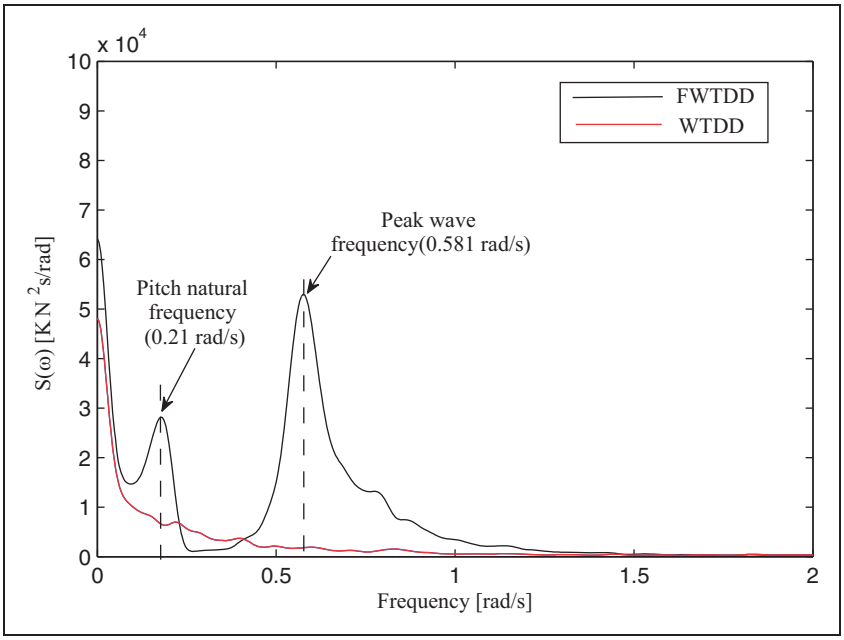

Figure 17. Frequency spectra of main shaft axial forces – FWTDD vs WTDD systems.
FWTDD: floating wind turbine with a direct-drive generator; WTDD: Land-based wind turbine with a direct-drive generator.

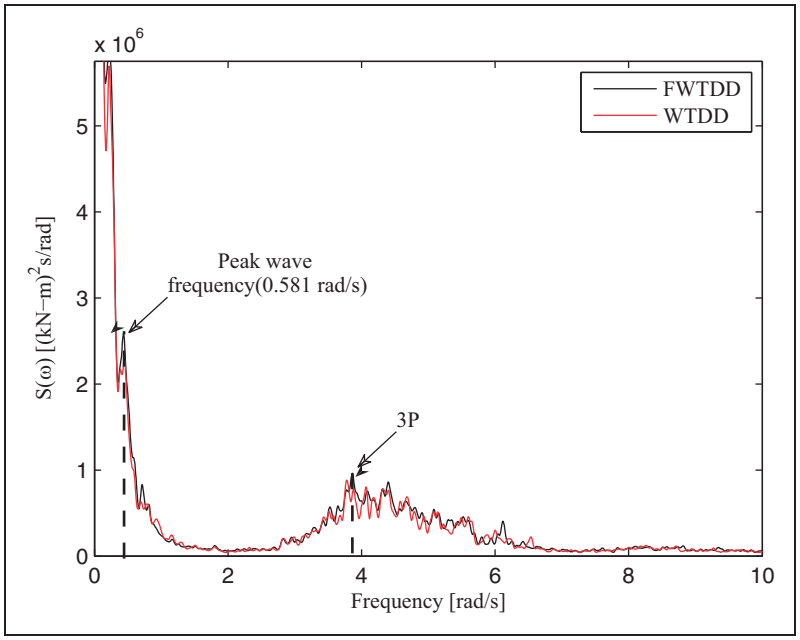

Figure 18. Frequency spectra of main shaft bending moments – FWTDD vs WTDD systems.
FWTDD: floating wind turbine with a direct-drive generator; WTDD: Land-based wind turbine with a direct-drive generator.

6 P frequencies. This could explain the reason for the larger standard deviations in shear forces. Likewise, the main shaft axial load spectra show excitations at wave frequency and the platform's pitch natural frequency. The frequency spectra for the bending moments are very similar for the FWTDD and WTDD system, which accounts for the relatively smaller variation in mean, standard deviation and maximum values. The main shaft torque load spectrum for the FWTDD system resembles that of WTDD system for most part with the exception of wave induced excitation. Thus, these load spectra suggest that the impact of wave excitation and platform's natural frequency can be felt by the load bearing components in the drive-train for the FWTDD system.

It must be remembered that HAWC2 simulations assume only a torsional degree of freedom for the main shaft system. However a real rotor-shaft assembly experiences 6 DOF motions; hence a multitude of response variables have to be analysed.

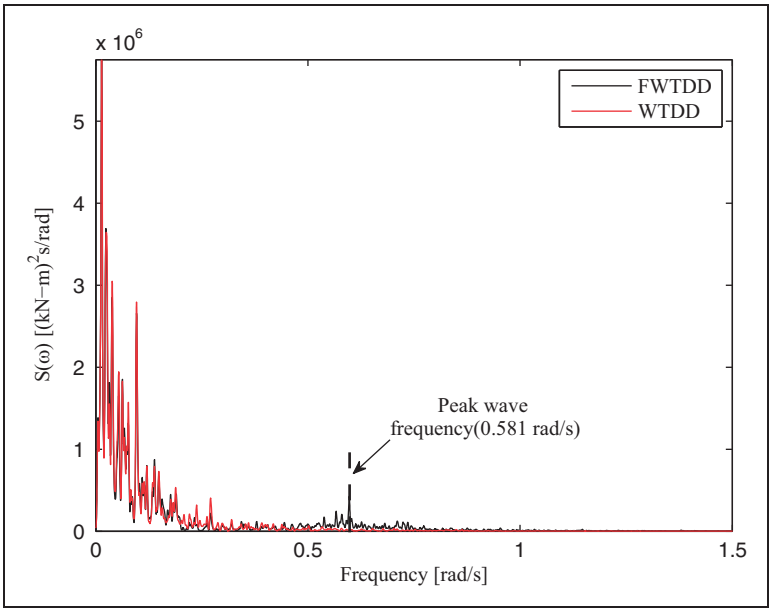

Figure 19. Frequency spectra of main shaft torque – FWTDD vs WTDD systems.
FWTDD: floating wind turbine with a direct-drive generator; WTDD: Land-based wind turbine with a direct-drive generator.

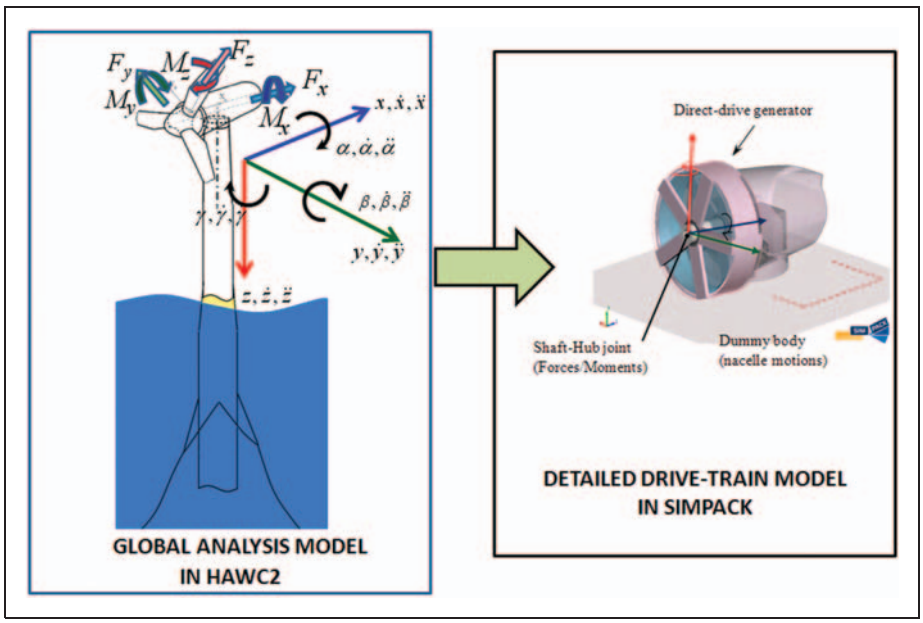

Figure 20. Drive-train analysis methodology, based on Xing et al.[10]

Therefore, interpretation of results from this study must be done with care and good sense of engineering judgement. This also obligates the need to evaluate the internal dynamic response of the generator, to make a detailed assessment.

Internal drive-train behaviour

In order to be able to assess the performance of the FWTDD system more closely, the detailed dynamic behaviour of the drive-train must be evaluated. Since the global model (in HAWC2) generally ignores the internal loading within the drive-train, another simulation model must be developed for detailed drive-train investigation. This can be subsequently used to verify the design loads, component durability and validate any assumptions for global load simulation (e.g. stiffness, mass etc.). Possible reactions expected from the direct-drive system include: (a) eccentricity-induced unbalanced magnetic pull[21,62] and (b) shaft vibrations that manifest as bearing load[63] and torsional vibrations in the drive-train.

Eccentricity effects particularly cause large stresses on bearings thereby reducing their lifetime. Torsional vibrations, on the other hand can trigger spurious pitch action and result in electrical power oscillations that can interact with the power system modes. In order to examine these sensitivities, a two-step decoupled approach proposed by Xing et al.[10] shall be used. Figure 20 shows the schematic diagram for this methodology. The global motion response and loads from HAWC2 are input to a detailed drive-train model in SIMPACK, a general purpose multi-body simulation (MBS) software that enables kinematic and dynamic analysis of mechanical systems.[15] The SIMPACK model is a stand-alone system with the properties of the drive-train model as described in section 'Development of drive-train mechanical properties', with the fundamental elements of the generator modelled using the topology described in Sethuraman et al.[62] This model however will be segregated from the tower, turbine and controller elements to allow for an independent analysis of the drive-train. The time series of 6 DOF motion response variables for position ($p(t)$, $\theta(t)$), velocity ($v(t)$, $\omega(t)$) and acceleration ($a(t)$, $\alpha(t)$) from HAWC2 simulations are kinematic inputs to the SIMPACK model. Shaft moments ($M_{x,y,z}$) and forces ($F_{x,y,z}$) are applied at the hub end where the turbine is assumed to be attached. The SIMPACK model will be used to examine the internal responses and loading of the drive-train which include bearing forces, shaft displacements, eccentricity and unbalanced magnetic pull (UMP).

Conclusions

The preliminary specifications for a floating version of 5 MW direct-drive wind turbine was developed for the purpose of carrying out fully coupled time-domain aero-hydro-servo-elastic simulations. The OC3-hywind model served as the main reference system to establish these specifications. Detailed drive-train properties including dimensions of the shaft, mechanical properties were developed to suit a radial flux permanent magnet generator topology that was obtained from previous optimisation studies. The direct-drive system made the nacelle heavier than the geared system requiring few adjustments to the design. The task involving adjustments to tower and platform properties revealed the challenge of maintaining the same draft as that of a geared system with larger nacelle mass. Yet, it was possible to match the resonance properties with that of geared FWT system by manipulating the location of power distribution/auxiliary equipment. This resulted in a slightly heavier tower, although rest of the system did not require any major modifications. The overall mass of the developed FWTDD system is generally consistent with existing spar designs. The behaviour of the model was tested for the normal operating conditions of the wind turbine using an aero-elastic modelling tool, HAWC2. The following were observed from the results of simulations:

(a) Considerable blade-pitch instability was observed for a controller response frequency of 0.125 rad/s. A more stable response was observed by tuning the frequency to a lower value at 0.09 rad/s, although the controller response was not optimised for all operating conditions.
(b) The motion response behaviour of the FWTDD system was found to be generally consistent with the typical response characteristics observed for the geared spar buoy wind turbine. This also helped to verify the consistency of the specifications developed for the aero-hydro-servo-elastic model.
(c) There is only a marginal variation of the mean, standard deviation and maximum values of bending moments and torques for the FWTDD system as compared to its land-based counterpart. This implies a negligible implication to power production which is a favourable attribute.
(d) Additional shaft axial loads and shear loads in the FWTDD system were caused by wave excitations and platform motions. The mean values were limited to less than 12%, but upto 35% increase in maximum axial loads were observed. This suggested an increase in bearing loads.

In summary, the aero-hydro-servo-elastic model developed in this study was useful in identifying the special structural requirements and design adjustments that might be necessary for accommodating a direct-drive generator for a FWT. The main shaft behaviour observed from fully coupled simulations for the FWTDD system in HAWC2 showed a moderate increase in loads thereby suggesting a satisfactory dynamic behaviour. With fewer rotating parts and wear components, it is expected that the direct-drive generator can promise greater reliability; so that any additional capital investments (on structural requirements) for the FWTDD system will be outweighed by the superior performance. Further investigations on the detailed internal drive-train behaviour must be carried out to verify this hypothesis and ascertain any further challenges/opportunities in implementing the direct-drive model for floating wind turbines.

Funding

The first author acknowledges funding from the University of Edinburgh through the Principal's career development scholarship and the Edinburgh Global Overseas Research scholarship programmes. This work was carried out in collaboration with the Department of Marine Technology, NTNU, Trondheim, Norway towards the MARINA Platform project, Grant Agreement no 241402, funded by the EC Seventh framework programme theme FP7 ENERGY.

Conflict of interest

None declared.

References

1. Floating Offshore Wind Foundations: Industry Consortia and Projects in the United States, Europe and Japan. May 2013 update. An Overview by Main(e) International Consulting LLC, http://maine-intl-consulting.com/resources/Floating+Offshore+Wind+Platforms+Consortia+for+web.pdf (accessed October 2013).
2. Jonkman JM. Dynamics modeling and loads analysis of an offshore floating wind turbine. NREL/TP-500-41958, November 2007.
3. Skaare B, Hanson TD, Nielsen FG, et al. Integrated dynamic analysis of floating offshore wind turbines. In: *European wind energy conference*, Milan, Italy, 2007.
4. Karimirad M and Moan T. Wave and wind induced dynamic response of a spar-type offshore wind turbine. *J Waterway Port Coastal Ocean Eng* 2012; 138: 9–20.
5. Robertson AN and Jonkman JM. Loads analysis of several offshore floating wind turbine concepts. In: *The international society of offshore and polar engineers conference*, Maui, Hawaii, 19–24 June 2011.
6. Utsunomiya T, Matsukuma H, Minoura S, et al. At sea experiment of a hybrid spar for floating offshore wind turbine using 1/10-scale model. *Offshore Mechanics and Arctic Engineering*, June 2013, p. 135.
7. Sethuraman L, Venugopal V and Mueller MA. Drive-train configurations for floating wind turbines: On the assessment of key design parameters and technology option. In: *Eighth international conference & exhibition on ecological vehicles and renewable energy*, Monte Carlo, 26–30 March 2013.
8. Link H, LaCava W, Van Dam J, et al. Gearbox reliability collaborative project report: Findings from Phase 1 and Phase 2 testing, NREL/TP-5000-51885, 2011.
9. Xing Y, Karimirad M and Moan T. Effect of spar-type floating wind turbine nacelle motion on drivetrain dynamics. In: *Proceedings of EWEA 2012 annual event*, Copenhagen, Denmark, 16–19 April 2012.
10. Xing Y, Karimirad M and Moan T. Modelling and analysis of floating spar-type wind turbine drivetrain. *Wind Energy* 2012: 1–23. DOI: 10.1002/we.
11. Advanced Wind Turbine Drive Train Concepts: Workshop report. US Department of Energy, Energy Efficiency and Renewable Energy, Wind and Water Program. NREL, Wind and Hydropower Technologies Program, www.nrel.gov/docs/fy11osti/50043.pdf (accessed October 2013).
12. Leban K, Ritchie E and Argeseanu A. Design preliminaries for direct drive underwater wind turbine generator, In: *XXth international conference on electrical machines (ICEM)*, Marseille, 2–5 September 2012.
13. Boulder Wind Power. Advanced Gearless Drivetrain - Phase I Technical Report. U.S. DOE Wind and Water Power Program, www.osti.gov/bridge/servlets/purl/1050994/ (accessed October 2013)
14. Larsen TJ and Hansen AM. How2 HAWC2. User Manual, Risø National Laboratory Riso-R-1597(ver. 4-3), Technical University of Denmark, Lyngby, Denmark, 2012.
15. Welcome to Simpack, http://www.simpack.com/ (accessed October 2013)
16. Dubois MR, Polinder H and Ferreira JA. Comparison of generator topologies for direct-drive wind turbines. In: *Proceedings of Nordic countries power & industrial electronics conference*, Aalborg, Denmark, June 2000.
17. Direct Drive (Gearless) Wind Turbine Market, By Permanent Magnet (PMSG) & Electrically Excited (EESG) Generator Technology, Turbine Size/Capacity Range - Global Trends & Forecasts to 2017, http://www.marketsandmarkets.com/Market-Reports/direct-drive-gearless-wind-turbine-market-805.html (accessed October 2013).
18. Bang D, Polinder H, Shrestha G, et al. Review of generator systems for direct drive wind turbines. In: *2008 European wind energy conference*, Brussels, 2008.
19. Paulsen US, Vita L, Madsen HA, et al. 1st DeepWind 5 MW baseline design. *Energy Procedia* 2012; 24: 27–35.
20. Borgen E. Introduction of the sway turbine ST10. In: *IQPC 3rd international conference drivetrain concepts for wind turbines*, Germany, 22–24 October 2012.
21. Sethuraman L, Venugopal V, Zavvos A, et al. Structural integrity of a direct-drive generator for a floating wind turbine. *Renew Energy* 2014; 63: 597–616.
22. Stander JN, Venter G and Kamper MJ. Review of direct drive radial flux permanent magnet generator mechanical design. *Wind Energy* 2012; 15: 459–472.
23. Poore R and Lettenmaier T. Alternative design study report: WindPACT advanced wind turbine drive train designs study, 2002.
24. Smith EB. Nacelle design for a 10MW reference wind turbine. M.S. Thesis, NTNU, 2012.
25. Jonkman J. Definition of the floating system for phase IV of OC3. NREL/TP-500-47535, May 2010.
26. Jonkman J, Butterfield S, Musial W, et al. Definition of a 5-MW reference wind turbine for offshore system development. NREL/TP-500-38060, February 2009.
27. Zavvos A, McDonald AS and Mueller M. Structural optimisation tools for iron cored permanent magnet generators for large direct-drive wind turbines. In: *Renewable power generation conference (RPG 2011)*, Edinburgh, UK, 6–8 September 2011.
28. Bang D and Polinder H. Electromagnetic optimization of direct-drive generators. Upwind Deliverable No.: D 1B2.b.hp2, www.upwind.eu/media/832/Deliverable_1B2.b.hp2.pdf (accessed October 2013).
29. http://www.mtoi.es/en/productos-y-servicios/index.aspx (accessed October 2013).
30. Spooner E, Gordon P and French CD. Lightweight, ironless-stator, PM generators for direct-drive wind turbines. In: *Second international conference on power electronics, machines and drives (PEMD)*, Edinburgh, 2004.
31. Turi MB and Marks CS. Bearing selection techniques as applied to main shaft direct and hybrid drives for wind turbines. TIMKEN Technical Paper, http://www.whereyouturn.com/ja-jp/about/NewsRoom/MediaKits/Documents/MainShaftTechPaper.pdf (accessed October 2013).
32. Jonkman JM. Dynamics modeling and loads analysis of an offshore floating wind turbine. PhD Thesis, University of Colorado-Boulder, 2007.
33. Fingersh L, Hand M and Laxson A. Wind turbine design cost and scaling model. NREL/TP-500-40566, 2006.

34. Malcolm DJ and Hansen AC. WindPACT turbine rotor design study June 2000–June 2002. NREL/SR-500-32495, Revised April 2006.
35. Kooijman HJT, Lindenburg C, Winkelaar D, et al. DOWEC 6 MW pre-design: Aero-elastic modeling of the DOWEC 6 MW pre-design in PHATAS DOWEC-F1W2-HJK-01-046/09, Energy Research Center of the Netherlands, September 2003.
36. SolidWorks 2013. http://www.solidworks.com/launch/solidworks-2013-overview.htm (accessed October 2013).
37. Hau E. *Vibration characteristics*. *Wind Turbines 2013*. Springer Berlin Heidelberg, 2013, pp.233–268.
38. Ferdinand P, Beer E, Russell Johnston J, et al. *Mechanics of materials*. New York: The McGraw-Hill Companies, 2002.
39. https://wind.nrel.gov/forum/wind/viewtopic.php?f=4&t=743 (accessed October 2013).
40. Versteegh Kivi CJA and Voordracht N. Direct driven generators in wind turbines: Experience with the 5 MW prototype. XEMC Darwind, 7 November 2011, https://afdelingen.kiviniria.net/media-afdelingen/DOM100000223/Verslagen_presentaties/2011/20111107_XEMC-Darwind_symposium/KeesV-Presentatie_Kivi_TUE_7112011.pdf (accessed July 2013).
41. http://www.goldwindamerica.com/technology-capabilities/2-5-mw-pmdd/ (accessed February 2014).
42. Johannessen K, Meling TS and Haver S. Joint distribution for wind and waves in the northern North Sea. In: *International Offshore and Polar Engineering Conference*, International Society of Offshore and Polar Engineers (ISOPE), Cupertino, CA, 2001.
43. Zavvos A, McDonald AS and Mueller MA. Optimized mechanical structures of direct-drive generators. Upwind Research report (Deliverable No.: D 1B2.b.5), http://www.upwind.eu/media/823/Deliverable_1B2.b.5.pdf (accessed August 2013).
44. Zavvos A, Bang D, McDonald AS, et al. Structural analysis and optimisation of transverse flux permanent magnet machines for 5 and 10 MW direct drive wind turbines. *Wind Energy* 2012; 15: 19–43.
45. McDonald AS and Mueller MA. A light-weight low speed permanent magnet electrical generator for direct-drive wind turbines. *Wind Energy* 2009; 12: 768–780.
46. Shrestha G. *Structural flexibility of large direct drive generators for wind turbines*. PhD Thesis, Delft University of Technology, 2013.
47. Maples B, Hand M and Musial W. Comparative assessment of direct drive high temperature superconducting generators in multi-megawatt class wind turbines. Technical Report NREL/TP-5000-49086, October 2010.
48. Matha D. Model development and loads analysis of an offshore wind turbine on a tension leg platform, with a comparison to other floating turbine concepts. NREL/SR-500-45891, 2009.
49. Jonkman JM and Buhl ML Jr. FAST user's guide, NREL/EL-500-38230, August 2005.
50. http://www.statoil.com/en/TechnologyInnovation/NewEnergy/RenewablePowerProduction/Offshore/Hywind/Downloads/Hywind%20Fact%20sheet.pdf (accessed October 2013).
51. Polinder H, Bang D, Van Rooij RPJOM, et al. 10 MW wind turbine direct-drive generator design with pitch or active speed stall control. In: *IEEE international electric machines & drives conference, IEMDC '07*, Antalya, 3–5 May 2007.
52. Johnson K, Fingersh L, Balas M, et al. Methods for increasing region 2 power capture on a variable speed HAWT. In: *Proceedings of the 23rd ASME wind energy symposium*, Reno, 2004.
53. Wright AD and Fingersh L. Advanced control design for wind turbines. Part I: Control design, implementation, and initial tests. NREL/TP-500-42437, March 2008.
54. Larsen TJ and Hanson TD. A method to avoid negative damped low frequent tower vibrations for a floating, pitch controlled wind turbine. *J Phys: Conf Ser* 2007. DOI:10.1088/1742-6596/75/1/012073.
55. Larsen TJ. A practical guide to tuning of a controller for a floating pitch regulated turbine. Risø National Laboratory, Technical University of Denmark, September 2007.
56. Mann J. Models in micrometeorology. Technical Report, Riso National Laboratory. 1994.
57. Faltinsen OM. *Sea loads on ships and offshore structures*. 1st ed. Cambridge: Cambridge University Press, 1990.
58. Karimirad M, Meissonnier Q, Gao Z, et al. Hydro-elastic code-to-code comparison for a tension leg spar-type floating wind turbine. *Marine Struct* 2011; 24: 412–435.
59. IEC 61400-3: *Design requirements for offshore wind turbines*. 1st ed., 2009.
60. Faltinsen OM. *Sea loads on ships and offshore structures*. 1st ed. Cambridge: Cambridge University Press, 1990.
61. Recommended Practice DNV-RP-C205. Environmental conditions and environmental loads, October 2010.
62. Sethuraman L, Xing Y, Gao Z, et al. A multi-body model of a direct drive generator for a wind turbine. In: *The proceedings of EWEA 2014*, Barcelona, 10–13 March 2014.
63. Whittle M, Trevelyan J and Wu J. A parametric study of the effect of generator misalignment on bearing fatigue life in wind turbines. In: *The proceedings of EWEA 2011,* Brussels, 14–17 March 2011.